Mean-Variance Analysis in Bayesian Optimization under Uncertainty: Supplementary Materials

Contents

A Proofs

A.1 Proof of Lemma 3.1

Proof. Let us consider the following event in Lemma 2.1:

$$\forall \boldsymbol{x} \in \mathcal{X},\ \forall \boldsymbol{w} \in \Omega,\ \forall t \geq 1,\ |f(\boldsymbol{x}, \boldsymbol{w}) - \mu_{t-1}(\boldsymbol{x}, \boldsymbol{w})| \leq \beta_t^{1/2} \sigma_{t-1}(\boldsymbol{x}, \boldsymbol{w}). \tag{7}$$

Under the event (7), the following holds:

$$\forall \boldsymbol{x} \in \mathcal{X},\ \forall t \geq 1,\ \int_\Omega l_t(\boldsymbol{x}, \boldsymbol{w}) p(\boldsymbol{w}) \mathrm{d}\boldsymbol{w} \leq \int_\Omega f(\boldsymbol{x}, \boldsymbol{w}) p(\boldsymbol{w}) \mathrm{d}\boldsymbol{w} \leq \int_\Omega u_t(\boldsymbol{x}, \boldsymbol{w}) p(\boldsymbol{w}) \mathrm{d}\boldsymbol{w}.$$

This indicates $F_1(\boldsymbol{x}) \in Q_t^{(F_1)}(\boldsymbol{x})$ for all $\boldsymbol{x} \in \mathcal{X}$, $t \geq 1$ under the event (7).

Next, we show that $F_2(\boldsymbol{x}) \in Q_t^{(F_2)}(\boldsymbol{x})$ holds for all $\boldsymbol{x} \in \mathcal{X}$, $t \geq 1$ under the event (7). Let us consider the quantity $f(\boldsymbol{x}, \boldsymbol{w}) - \mathbb{E}_{\boldsymbol{w}}[f(\boldsymbol{x}, \boldsymbol{w})]$, which appears in the integrand of $\mathbb{V}_{\boldsymbol{w}}[f(\boldsymbol{x}, \boldsymbol{w})]$. Under the event (7), the following holds:

$$\forall \boldsymbol{x} \in \mathcal{X},\ \forall t \geq 1,\ \tilde{l}_t(\boldsymbol{x}, \boldsymbol{w}) \leq f(\boldsymbol{x}, \boldsymbol{w}) - \mathbb{E}_{\boldsymbol{w}}[f(\boldsymbol{x}, \boldsymbol{w})] \leq \tilde{u}_t(\boldsymbol{x}, \boldsymbol{w}), \tag{8}$$

where $\tilde{l}_t(\boldsymbol{x}, \boldsymbol{w}) = l_t(\boldsymbol{x}, \boldsymbol{w}) - \mathbb{E}_{\boldsymbol{w}}[u_t(\boldsymbol{x}, \boldsymbol{w})]$ and $\tilde{u}_t(\boldsymbol{x}, \boldsymbol{w}) = u_t(\boldsymbol{x}, \boldsymbol{w}) - \mathbb{E}_{\boldsymbol{w}}[l_t(\boldsymbol{x}, \boldsymbol{w})]$. Regarding to the integrand of $\mathbb{V}_{\boldsymbol{w}}[f(\boldsymbol{x}, \boldsymbol{w})]$, the following inequality holds for all $\boldsymbol{x} \in \mathcal{X}$, $t \geq 1$ when (8) holds:

$$\tilde{l}_t^{(\mathrm{sq})}(\boldsymbol{x}, \boldsymbol{w}) \leq \{f(\boldsymbol{x}, \boldsymbol{w}) - \mathbb{E}_{\boldsymbol{w}}[f(\boldsymbol{x}, \boldsymbol{w})]\}^2 \leq \tilde{u}_t^{(\mathrm{sq})}(\boldsymbol{x}, \boldsymbol{w}), \tag{9}$$

where

$$\tilde{l}_t^{(\mathrm{sq})}(\boldsymbol{x}, \boldsymbol{w}) = \begin{cases} 0 & \text{if } \tilde{l}_t(\boldsymbol{x}, \boldsymbol{w}) \leq 0 \leq \tilde{u}_t(\boldsymbol{x}, \boldsymbol{w}), \\ \min\left\{\tilde{l}_t^2(\boldsymbol{x}, \boldsymbol{w}), \tilde{u}_t^2(\boldsymbol{x}, \boldsymbol{w})\right\} & \text{otherwise} \end{cases},$$
$$\tilde{u}_t^{(\mathrm{sq})}(\boldsymbol{x}, \boldsymbol{w}) = \max\left\{\tilde{l}_t^2(\boldsymbol{x}, \boldsymbol{w}), \tilde{u}_t^2(\boldsymbol{x}, \boldsymbol{w})\right\}.$$

The inequality (9) is derived from the fact that, for any a, b $(a \leq b)$,

$$a \leq x \leq b \Rightarrow \tilde{a} \leq x^2 \leq \tilde{b}$$

where

$$\tilde{a} = \begin{cases} 0 & \text{if } a \leq 0 \leq b, \\ \min\{a^2, b^2\} & \text{otherwise} \end{cases},$$
$$\tilde{b} = \max\{a^2, b^2\}.$$

Finally, from the monotonicity of square root and the definition of $Q_t^{(F_2)}(\boldsymbol{x})$, $F_2(\boldsymbol{x}) \in Q_t^{(F_2)}(\boldsymbol{x})$ holds for all $\boldsymbol{x} \in \mathcal{X}$, $t \geq 1$ under the event (7). From Lemma 2.1 and the definition of β_t, the event (7) holds with probability at least $1 - \delta$. Therefore, with probability at least $1 - \delta$, $F_1(\boldsymbol{x}) \in Q_t^{(F_1)}(\boldsymbol{x})$ and $F_2(\boldsymbol{x}) \in Q_t^{(F_2)}(\boldsymbol{x})$ holds for any $\boldsymbol{x} \in \mathcal{X}, t \geq 1$. ■

A.2 Proof of Theorem 4.1

From the definition of β_t and Lemma 2.1, the following holds with probability at least $1 - \delta/3$:

$$\forall\ \boldsymbol{x} \in \mathcal{X},\ \forall \boldsymbol{w} \in \Omega,\ \forall t \geq 1,\ |f(\boldsymbol{x}, \boldsymbol{w}) - \mu_{t-1}(\boldsymbol{x}, \boldsymbol{w})| \leq \beta_t^{1/2} \sigma_{t-1}(\boldsymbol{x}, \boldsymbol{w}). \tag{10}$$

Moreover, we give the following lemma about the confidence bound $Q_t^{(G)}(\boldsymbol{x}_t)$:

Lemma A.1. *Assume that (10) holds. Then, for any $T \geq 1$, it holds that*

$$\sum_{t=1}^T \left\{u_t^{(G)}(\boldsymbol{x}_t) - l_t^{(G)}(\boldsymbol{x}_t)\right\} \leq 2\alpha\beta_T^{1/2} \sum_{t=1}^T \int_\Omega \sigma_{t-1}(\boldsymbol{x}_t, \boldsymbol{w}) p(\boldsymbol{w}) \mathrm{d}\boldsymbol{w}$$
$$+ (1 - \alpha)\sqrt{8T\tilde{B}\beta_T^{1/2} \sum_{t=1}^T \int_\Omega \sigma_{t-1}(\boldsymbol{x}_t, \boldsymbol{w}) p(\boldsymbol{w}) \mathrm{d}\boldsymbol{w} + 20T\beta_T \sum_{t=1}^T \int_\Omega \sigma_{t-1}^2(\boldsymbol{x}_t, \boldsymbol{w}) p(\boldsymbol{w}) \mathrm{d}\boldsymbol{w}},$$

where $\tilde{B} = \max_{(\boldsymbol{x}, \boldsymbol{w}) \in (\mathcal{X} \times \Omega)} |f(\boldsymbol{x}, \boldsymbol{w}) - \mathbb{E}_{\boldsymbol{w}}[f(\boldsymbol{x}, \boldsymbol{w})]|$.

Proof. From the definition of $u_t^{(G)}$ and $l_t^{(G)}$, we have

$$\sum_{t=1}^{T} \left\{ u_t^{(G)}(\boldsymbol{x}_t) - l_t^{(G)}(\boldsymbol{x}_t) \right\} = \alpha \sum_{t=1}^{T} \left\{ u_t^{(F_1)}(\boldsymbol{x}_t) - l_t^{(F_1)}(\boldsymbol{x}_t) \right\} + (1-\alpha) \sum_{t=1}^{T} \left\{ u_t^{(F_2)}(\boldsymbol{x}_t) - l_t^{(F_2)}(\boldsymbol{x}_t) \right\}. \tag{11}$$

Similarly, from the definition of $u_t^{(F_1)}$ and $l_t^{(F_1)}$, we get the following inequality:

$$\begin{aligned} \sum_{t=1}^{T} \left\{ u_t^{(F_1)}(\boldsymbol{x}_t) - l_t^{(F_1)}(\boldsymbol{x}_t) \right\} &= \sum_{t=1}^{T} \int_\Omega \{ u_t(\boldsymbol{x}_t, \boldsymbol{w}) - l_t(\boldsymbol{x}_t, \boldsymbol{w}) \} p(\boldsymbol{w}) \mathrm{d}\boldsymbol{w} \\ &= 2 \sum_{t=1}^{T} \beta_t^{1/2} \int_\Omega \sigma_{t-1}(\boldsymbol{x}_t, \boldsymbol{w}) p(\boldsymbol{w}) \mathrm{d}\boldsymbol{w} \\ &\le 2 \beta_T^{1/2} \sum_{t=1}^{T} \int_\Omega \sigma_{t-1}(\boldsymbol{x}_t, \boldsymbol{w}) p(\boldsymbol{w}) \mathrm{d}\boldsymbol{w}. \end{aligned} \tag{12}$$

Here, the last inequality is given by monotonicity of β_t. In addition, noting that the definition of $u_t^{(F_2)}$ and $l_t^{(F_2)}$ we obtain

$$\begin{aligned} u_t^{(F_2)}(\boldsymbol{x}_t) - l_t^{(F_2)}(\boldsymbol{x}_t) &= \sqrt{\int_\Omega \tilde{u}_t^{(\mathrm{sq})}(\boldsymbol{x}_t, \boldsymbol{w}) p(\boldsymbol{w}) \mathrm{d}\boldsymbol{w}} - \sqrt{\int_\Omega \tilde{l}_t^{(\mathrm{sq})}(\boldsymbol{x}_t, \boldsymbol{w}) p(\boldsymbol{w}) \mathrm{d}\boldsymbol{w}} \\ &\le \sqrt{\int_\Omega \left\{ \tilde{u}_t^{(\mathrm{sq})}(\boldsymbol{x}_t, \boldsymbol{w}) - \tilde{l}_t^{(\mathrm{sq})}(\boldsymbol{x}_t, \boldsymbol{w}) \right\} p(\boldsymbol{w}) \mathrm{d}\boldsymbol{w}}, \end{aligned} \tag{13}$$

where the last inequality is obtained by using the fact that $\sqrt{a} - \sqrt{b} \le \sqrt{a-b}$ for any $a \ge b \ge 0$. Furthermore, we have

$$\tilde{u}_t^{(\mathrm{sq})}(\boldsymbol{x}_t, \boldsymbol{w}) - \tilde{l}_t^{(\mathrm{sq})}(\boldsymbol{x}_t, \boldsymbol{w}) = \max \left\{ \tilde{l}_t^2(\boldsymbol{x}_t, \boldsymbol{w}), \tilde{u}_t^2(\boldsymbol{x}_t, \boldsymbol{w}) \right\} - \min \left\{ \tilde{l}_t^2(\boldsymbol{x}_t, \boldsymbol{w}), \tilde{u}_t^2(\boldsymbol{x}_t, \boldsymbol{w}) \right\} + \mathrm{STR}_{0,t}^2(\boldsymbol{x}_t, \boldsymbol{w}), \tag{14}$$

where $\mathrm{STR}_{0,t}(\boldsymbol{x}_t, \boldsymbol{w}) = \max \left\{ 0, \min \left(\tilde{u}_t(\boldsymbol{x}_t, \boldsymbol{w}), -\tilde{l}_t(\boldsymbol{x}_t, \boldsymbol{w}) \right) \right\}$. Moreover, we define $\tilde{\mu}_{t-1}(\boldsymbol{x}, \boldsymbol{w})$ and $\tilde{\sigma}_{t-1}(\boldsymbol{x}, \boldsymbol{w})$ as

$$\begin{aligned} \tilde{\mu}_{t-1}(\boldsymbol{x}, \boldsymbol{w}) &= \mu_{t-1}(\boldsymbol{x}, \boldsymbol{w}) - \mathbb{E}_{\boldsymbol{w}}[\mu_{t-1}(\boldsymbol{x}, \boldsymbol{w})], \\ \tilde{\sigma}_{t-1}(\boldsymbol{x}, \boldsymbol{w}) &= \sigma_{t-1}(\boldsymbol{x}, \boldsymbol{w}) + \mathbb{E}_{\boldsymbol{w}}[\sigma_{t-1}(\boldsymbol{x}, \boldsymbol{w})]. \end{aligned}$$

Then, $\tilde{l}_t(\boldsymbol{x}, \boldsymbol{w})$ and $\tilde{u}_t(\boldsymbol{x}, \boldsymbol{w})$ can be expressed as follows:

$$\begin{aligned} \tilde{l}_t(\boldsymbol{x}, \boldsymbol{w}) &= \tilde{\mu}_{t-1}(\boldsymbol{x}, \boldsymbol{w}) - \beta_t^{1/2} \tilde{\sigma}_{t-1}(\boldsymbol{x}, \boldsymbol{w}), \\ \tilde{u}_t(\boldsymbol{x}, \boldsymbol{w}) &= \tilde{\mu}_{t-1}(\boldsymbol{x}, \boldsymbol{w}) + \beta_t^{1/2} \tilde{\sigma}_{t-1}(\boldsymbol{x}, \boldsymbol{w}). \end{aligned}$$

Here, if $\tilde{l}_t^2(\boldsymbol{x}_t, \boldsymbol{w}) \le \tilde{u}_t^2(\boldsymbol{x}_t, \boldsymbol{w})$, then we have $\tilde{\mu}_{t-1}(\boldsymbol{x}_t, \boldsymbol{w}) \ge 0$ and

$$\begin{aligned} &\max \left\{ \tilde{l}_t^2(\boldsymbol{x}_t, \boldsymbol{w}), \tilde{u}_t^2(\boldsymbol{x}_t, \boldsymbol{w}) \right\} - \min \left\{ \tilde{l}_t^2(\boldsymbol{x}_t, \boldsymbol{w}), \tilde{u}_t^2(\boldsymbol{x}_t, \boldsymbol{w}) \right\} \\ &= \left\{ \tilde{\mu}_{t-1}(\boldsymbol{x}_t, \boldsymbol{w}) + \beta_t^{1/2} \tilde{\sigma}_{t-1}(\boldsymbol{x}_t, \boldsymbol{w}) \right\}^2 - \left\{ \tilde{\mu}_{t-1}(\boldsymbol{x}_t, \boldsymbol{w}) - \beta_t^{1/2} \tilde{\sigma}_{t-1}(\boldsymbol{x}_t, \boldsymbol{w}) \right\}^2 \\ &= 4 \beta_t^{1/2} \tilde{\mu}_{t-1}(\boldsymbol{x}_t, \boldsymbol{w}) \tilde{\sigma}_{t-1}(\boldsymbol{x}_t, \boldsymbol{w}) \\ &= 4 \beta_t^{1/2} |\tilde{\mu}_{t-1}(\boldsymbol{x}_t, \boldsymbol{w})| \tilde{\sigma}_{t-1}(\boldsymbol{x}_t, \boldsymbol{w}). \end{aligned}$$

On the other hand, if $\tilde{l}_t^2(\boldsymbol{x}_t, \boldsymbol{w}) > \tilde{u}_t^2(\boldsymbol{x}_t, \boldsymbol{w})$, then we get $\tilde{\mu}_{t-1}(\boldsymbol{x}_t, \boldsymbol{w}) < 0$ and

$$\begin{aligned} &\max \left\{ \tilde{l}_t^2(\boldsymbol{x}_t, \boldsymbol{w}), \tilde{u}_t^2(\boldsymbol{x}_t, \boldsymbol{w}) \right\} - \min \left\{ \tilde{l}_t^2(\boldsymbol{x}_t, \boldsymbol{w}), \tilde{u}_t^2(\boldsymbol{x}_t, \boldsymbol{w}) \right\} \\ &= \left\{ \tilde{\mu}_{t-1}(\boldsymbol{x}_t, \boldsymbol{w}) - \beta_t^{1/2} \tilde{\sigma}_{t-1}(\boldsymbol{x}_t, \boldsymbol{w}) \right\}^2 - \left\{ \tilde{\mu}_{t-1}(\boldsymbol{x}_t, \boldsymbol{w}) + \beta_t^{1/2} \tilde{\sigma}_{t-1}(\boldsymbol{x}_t, \boldsymbol{w}) \right\}^2 \\ &= -4 \beta_t^{1/2} \tilde{\mu}_{t-1}(\boldsymbol{x}_t, \boldsymbol{w}) \tilde{\sigma}_{t-1}(\boldsymbol{x}_t, \boldsymbol{w}) \\ &= 4 \beta_t^{1/2} |\tilde{\mu}_{t-1}(\boldsymbol{x}_t, \boldsymbol{w})| \tilde{\sigma}_{t-1}(\boldsymbol{x}_t, \boldsymbol{w}). \end{aligned}$$

Therefore, in all cases the following equality holds:

$$\max\left\{\tilde{l}_t^2(\boldsymbol{x}_t,\boldsymbol{w}),\tilde{u}_t^2(\boldsymbol{x}_t,\boldsymbol{w})\right\}-\min\left\{\tilde{l}_t^2(\boldsymbol{x}_t,\boldsymbol{w}),\tilde{u}_t^2(\boldsymbol{x}_t,\boldsymbol{w})\right\}=4\beta_t^{1/2}|\tilde{\mu}_{t-1}(\boldsymbol{x}_t,\boldsymbol{w})|\tilde{\sigma}_{t-1}(\boldsymbol{x}_t,\boldsymbol{w}).$$

Next, since (10) holds, we get $f(\boldsymbol{x},\boldsymbol{w})-\mathbb{E}_{\boldsymbol{w}}[f(\boldsymbol{x}_t,\boldsymbol{w})]\in[\tilde{l}_t(\boldsymbol{x},\boldsymbol{w}),\tilde{u}_t(\boldsymbol{x},\boldsymbol{w})]$. This implies that

$$|f(\boldsymbol{x},\boldsymbol{w})-\mathbb{E}_{\boldsymbol{w}}[f(\boldsymbol{x}_t,\boldsymbol{w})]-\tilde{\mu}_{t-1}(\boldsymbol{x},\boldsymbol{w})|\le\beta_t^{1/2}\tilde{\sigma}(\boldsymbol{x},\boldsymbol{w}).$$

Hence, we have

$$\begin{aligned}&|f(\boldsymbol{x},\boldsymbol{w})-\mathbb{E}_{\boldsymbol{w}}[f(\boldsymbol{x}_t,\boldsymbol{w})]-\tilde{\mu}_{t-1}(\boldsymbol{x},\boldsymbol{w})|\le\beta_t^{1/2}\tilde{\sigma}_{t-1}(\boldsymbol{x},\boldsymbol{w})\\ \Rightarrow\ &|\tilde{\mu}_{t-1}(\boldsymbol{x},\boldsymbol{w})|\le|f(\boldsymbol{x},\boldsymbol{w})-\mathbb{E}_{\boldsymbol{w}}[f(\boldsymbol{x}_t,\boldsymbol{w})]|+\beta_t^{1/2}\tilde{\sigma}_{t-1}(\boldsymbol{x},\boldsymbol{w})\\ \Rightarrow\ &|\tilde{\mu}_{t-1}(\boldsymbol{x},\boldsymbol{w})|\le\tilde{B}+\beta_t^{1/2}\tilde{\sigma}_{t-1}(\boldsymbol{x},\boldsymbol{w}).\end{aligned}$$

Thus, the following inequality holds:

$$\begin{aligned}&\max\left\{\tilde{l}_t^2(\boldsymbol{x}_t,\boldsymbol{w}),\tilde{u}_t^2(\boldsymbol{x}_t,\boldsymbol{w})\right\}-\min\left\{\tilde{l}_t^2(\boldsymbol{x}_t,\boldsymbol{w}),\tilde{u}_t^2(\boldsymbol{x}_t,\boldsymbol{w})\right\}\\ &\le4\beta_t^{1/2}\tilde{\sigma}_{t-1}(\boldsymbol{x}_t,\boldsymbol{w})\left\{\tilde{B}+\beta_t^{1/2}\tilde{\sigma}_{t-1}(\boldsymbol{x}_t,\boldsymbol{w})\right\}\\ &=4\tilde{B}\beta_t^{1/2}\tilde{\sigma}_{t-1}(\boldsymbol{x}_t,\boldsymbol{w})+4\beta_t\tilde{\sigma}_{t-1}^2(\boldsymbol{x}_t,\boldsymbol{w}).\end{aligned}\tag{15}$$

Moreover, $\mathrm{STR}_{0,t}(\boldsymbol{x}_t,\boldsymbol{w})$ can be bounded as

$$\begin{aligned}\mathrm{STR}_{0,t}(\boldsymbol{x}_t,\boldsymbol{w})&\le\frac{\tilde{u}_t(\boldsymbol{x}_t,\boldsymbol{w})-\tilde{l}_t(\boldsymbol{x}_t,\boldsymbol{w})}{2}\\ &=\beta_t^{1/2}\tilde{\sigma}_{t-1}(\boldsymbol{x}_t,\boldsymbol{w}).\end{aligned}\tag{16}$$

Hence, from (14), (15) and (16), we obtain

$$u_t^{(\mathrm{sq})}(\boldsymbol{x}_t,\boldsymbol{w})-l_t^{(\mathrm{sq})}(\boldsymbol{x}_t,\boldsymbol{w})\le4\tilde{B}\beta_t^{1/2}\tilde{\sigma}_{t-1}(\boldsymbol{x}_t,\boldsymbol{w})+5\beta_t\tilde{\sigma}_{t-1}^2(\boldsymbol{x}_t,\boldsymbol{w})$$

and

$$\begin{aligned}&\int_\Omega\left\{u_t^{(\mathrm{sq})}(\boldsymbol{x}_t,\boldsymbol{w})-l_t^{(\mathrm{sq})}(\boldsymbol{x}_t,\boldsymbol{w})\right\}p(\boldsymbol{w})\mathrm{d}\boldsymbol{w}\\ &\le4\tilde{B}\beta_t^{1/2}\int_\Omega\tilde{\sigma}_{t-1}(\boldsymbol{x}_t,\boldsymbol{w})p(\boldsymbol{w})\mathrm{d}\boldsymbol{w}+5\beta_t\int_\Omega\tilde{\sigma}_{t-1}^2(\boldsymbol{x}_t,\boldsymbol{w})p(\boldsymbol{w})\mathrm{d}\boldsymbol{w}.\end{aligned}$$

In addition, from the definition of $\tilde{\sigma}_{t-1}(\boldsymbol{x}_t,\boldsymbol{w})$, the following holds:

$$\begin{aligned}\int_\Omega\tilde{\sigma}_{t-1}(\boldsymbol{x}_t,\boldsymbol{w})p(\boldsymbol{w})\mathrm{d}\boldsymbol{w}&=\mathbb{E}_{\boldsymbol{w}}[\sigma_{t-1}(\boldsymbol{x}_t,\boldsymbol{w})]+\int_\Omega\sigma_{t-1}(\boldsymbol{x}_t,\boldsymbol{w})p(\boldsymbol{w})\mathrm{d}\boldsymbol{w}\\ &=2\int_\Omega\sigma_{t-1}(\boldsymbol{x}_t,\boldsymbol{w})p(\boldsymbol{w})\mathrm{d}\boldsymbol{w},\\ \int_\Omega\tilde{\sigma}_{t-1}^2(\boldsymbol{x}_t,\boldsymbol{w})p(\boldsymbol{w})\mathrm{d}\boldsymbol{w}&=\int_\Omega\sigma_{t-1}^2(\boldsymbol{x}_t,\boldsymbol{w})p(\boldsymbol{w})\mathrm{d}\boldsymbol{w}+2\mathbb{E}_{\boldsymbol{w}}[\sigma_{t-1}(\boldsymbol{x}_t,\boldsymbol{w})]\int_\Omega\sigma_{t-1}(\boldsymbol{x}_t,\boldsymbol{w})p(\boldsymbol{w})\mathrm{d}\boldsymbol{w}+\{\mathbb{E}_{\boldsymbol{w}}[\sigma_{t-1}(\boldsymbol{x}_t,\boldsymbol{w})]\}^2\\ &=\int_\Omega\sigma_{t-1}^2(\boldsymbol{x}_t,\boldsymbol{w})p(\boldsymbol{w})\mathrm{d}\boldsymbol{w}+3\left\{\int_\Omega\sigma_{t-1}(\boldsymbol{x}_t,\boldsymbol{w})p(\boldsymbol{w})\mathrm{d}\boldsymbol{w}\right\}^2\\ &\le4\int_\Omega\sigma_{t-1}^2(\boldsymbol{x}_t,\boldsymbol{w})p(\boldsymbol{w})\mathrm{d}\boldsymbol{w}.\end{aligned}$$

Here, the last inequality is obtained by using Jensen's inequality and convexity of $g(x)=x^2$. Therefore, we have

$$\begin{aligned}&\int_\Omega\left\{u_t^{(\mathrm{sq})}(\boldsymbol{x}_t,\boldsymbol{w})-l_t^{(\mathrm{sq})}(\boldsymbol{x}_t,\boldsymbol{w})\right\}p(\boldsymbol{w})\mathrm{d}\boldsymbol{w}\\ &\le8\tilde{B}\beta_t^{1/2}\int_\Omega\sigma_{t-1}(\boldsymbol{x}_t,\boldsymbol{w})p(\boldsymbol{w})\mathrm{d}\boldsymbol{w}+20\beta_t\int_\Omega\sigma_{t-1}^2(\boldsymbol{x}_t,\boldsymbol{w})p(\boldsymbol{w})\mathrm{d}\boldsymbol{w}.\end{aligned}\tag{17}$$

Thus, by using (17) and Schwartz's inequality for (13), we get

$$\sum_{t=1}^{T}\left\{u_t^{(F_2)}(\boldsymbol{x}_t)-l_t^{(F_2)}(\boldsymbol{x}_t)\right\}$$
$$\leq \sqrt{8T\tilde{B}\beta_T^{1/2}\sum_{t=1}^{T}\int_{\Omega}\sigma_{t-1}(\boldsymbol{x}_t,\boldsymbol{w})p(\boldsymbol{w})\mathrm{d}\boldsymbol{w}+20T\beta_T\sum_{t=1}^{T}\int_{\Omega}\sigma_{t-1}^2(\boldsymbol{x}_t,\boldsymbol{w})p(\boldsymbol{w})\mathrm{d}\boldsymbol{w}}. \tag{18}$$

Therefore, from (11), (12) and (18), we have the desired inequality. ∎

Next, in order to evaluate $\sum_{t=1}^{T}\int_{\Omega}\sigma_{t-1}(\boldsymbol{x}_t,\boldsymbol{w})\mathrm{d}\boldsymbol{w}$ and $\sum_{t=1}^{T}\int_{\Omega}\sigma_{t-1}^2(\boldsymbol{x}_t,\boldsymbol{w})\mathrm{d}\boldsymbol{w}$ in the right hand side of the inequality of Lemma A.1, we introduce the following lemma given by Kirschner and Krause (2018):

Lemma A.2. *Let S_t be any non-negative stochastic process adapted to a filtration $\{\mathcal{F}_t\}$, and define $m_t=E[S_t\mid\mathcal{F}_{t-1}]$. Assume that $S_t\leq K$ for $K\geq 1$. Then, for any $T\geq 1$, the following holds with probability at least $1-\delta$:*

$$\sum_{t=1}^{T}m_t\leq 2\sum_{t=1}^{T}S_t+8K\ln\frac{6K}{\delta}.$$

Furthermore, from the assumption about the kernel function, we get $k((\boldsymbol{x}_t,\boldsymbol{w}),(\boldsymbol{x}_t,\boldsymbol{w}))\leq 1$ and $\sigma_{t-1}(\boldsymbol{x}_t,\boldsymbol{w})\leq k((\boldsymbol{x}_t,\boldsymbol{w}),(\boldsymbol{x}_t,\boldsymbol{w}))\leq 1$. Hence, from Lemma A.2, with probability at least $1-\delta/3$, it holds that

$$\sum_{t=1}^{T}\int_{\Omega}\sigma_{t-1}(\boldsymbol{x}_t,\boldsymbol{w})p(\boldsymbol{w})\mathrm{d}\boldsymbol{w}\leq 2\sum_{t=1}^{T}\sigma_{t-1}(\boldsymbol{x}_t,\boldsymbol{w}_t)+8\ln\frac{18}{\delta}. \tag{19}$$

Similarly, the following inequality holds with probability at least $1-\delta/3$:

$$\sum_{t=1}^{T}\int_{\Omega}\sigma_{t-1}^2(\boldsymbol{x}_t,\boldsymbol{w})p(\boldsymbol{w})\mathrm{d}\boldsymbol{w}\leq 2\sum_{t=1}^{T}\sigma_{t-1}^2(\boldsymbol{x}_t,\boldsymbol{w}_t)+8\ln\frac{18}{\delta}. \tag{20}$$

In addition, we introduce the following lemma given by Srinivas et al. (2010) about the maximum information gain γ_T:

Lemma A.3. *Fix $T\geq 1$. Then, the following inequality holds:*

$$\sum_{t=1}^{T}\sigma_{t-1}^2(\boldsymbol{x}_t,\boldsymbol{w}_t)\leq\frac{2}{\ln(1+\sigma^{-2})}\gamma_T. \tag{21}$$

Moreover, from Schwarz's inequality and Lemma A.3, we get the following inequality:

$$\sum_{t=1}^{T}\sigma_{t-1}(\boldsymbol{x}_t,\boldsymbol{w}_t)\leq\sqrt{\frac{2T}{\ln(1+\sigma^{-2})}\gamma_T}. \tag{22}$$

Thus, from (19), (20), (21) and (22) we obtain the following corollary:

Corollary A.1. *Assume that (10), (19) and (20) hold. Then, for any $T\geq 1$, it holds that*

$$\sum_{t=1}^{T}\left\{u_t^{(G)}(\boldsymbol{x}_t)-l_t^{(G)}(\boldsymbol{x}_t)\right\}\leq\alpha\beta_T^{1/2}\left\{\sqrt{2TC_1\gamma_T}+C_2\right\}$$
$$+(1-\alpha)\sqrt{2T\tilde{B}\beta_T^{1/2}\left\{\sqrt{8TC_1\gamma_T}+2C_2\right\}+5T\beta_T\left\{C_1\gamma_T+2C_2\right\}},$$

where $C_1=\frac{16}{\ln(1+\sigma^{-2})}$ and $C_2=16\ln\frac{18}{\delta}$.

Proof. From Lemma A.1, (19) and (20), it holds that

$$\sum_{t=1}^{T}\left\{u_t^{(G)}(\boldsymbol{x}_t)-l_t^{(G)}(\boldsymbol{x}_t)\right\}\leq 4\alpha\beta_T^{1/2}\left\{\sum_{t=1}^{T}\sigma_{t-1}(\boldsymbol{x}_t,\boldsymbol{w}_t)+4\ln\frac{18}{\delta}\right\}$$
$$+(1-\alpha)\sqrt{16T\tilde{B}\beta_T^{1/2}\left\{\sum_{t=1}^{T}\sigma_{t-1}(\boldsymbol{x}_t,\boldsymbol{w}_t)+4\ln\frac{18}{\delta}\right\}+40T\beta_T\left\{\sum_{t=1}^{T}\sigma_{t-1}^2(\boldsymbol{x}_t,\boldsymbol{w}_t)+4\ln\frac{18}{\delta}\right\}}. \tag{23}$$

Therefore, by combining (21), (22) and (23), we get the desired inequality. ■

Finally, we prove Theorem 4.1. Let $T\geq 1$, and define $\hat{T}=\mathrm{argmax}_{t=1,\ldots,T}l_t^{(G)}(\boldsymbol{x}_t)$. Assume that (10) holds. Then, for any $\boldsymbol{x}\in\mathcal{X}$, it holds that $G(\boldsymbol{x})\in[l_t^{(G)}(\boldsymbol{x}),u_t^{(G)}(\boldsymbol{x})]$. Thus, for any $t'=1,\ldots,T$, we get

$$\begin{aligned}G(\boldsymbol{x}^*)-G(\hat{\boldsymbol{x}}_T)&\leq u_{t'}^{(G)}(\boldsymbol{x}_{t'})-l_{\hat{T}}^{(G)}(\hat{\boldsymbol{x}}_T)\\&=u_{t'}^{(G)}(\boldsymbol{x}_{t'})-\max_{t=1,\ldots,T}l_t^{(G)}(\hat{\boldsymbol{x}}_t)\\&\leq u_{t'}^{(G)}(\boldsymbol{x}_{t'})-l_{t'}^{(G)}(\boldsymbol{x}_{t'}).\end{aligned}$$

This implies that

$$G(\boldsymbol{x}^*)-G(\hat{\boldsymbol{x}}_T)\leq\frac{1}{T}\sum_{t=1}^{T}\left\{u_t^{(G)}(\boldsymbol{x}_t)-l_t^{(G)}(\boldsymbol{x}_t)\right\}. \tag{24}$$

Here, note that with probability at least $1-\delta$, (10), (19) and (20) hold. Therefore, by combining Corollary A.1, the following holds with probability at least $1-\delta$:

$$G(\boldsymbol{x}^*)-G(\hat{\boldsymbol{x}}_T)\leq\alpha T^{-1}\beta_T^{1/2}\left(\sqrt{2TC_1\gamma_T}+C_2\right)+(1-\alpha)T^{-1}\sqrt{2T\tilde{B}\beta_T^{1/2}\left(\sqrt{8TC_1\gamma_T}+2C_2\right)+5T\beta_T\left(C_1\gamma_T+2C_2\right)}.$$

Hence, if T satisfies $R_T/T\leq\epsilon$, with probability at least $1-\delta$, it holds that $G(\boldsymbol{x}^*)-G(\hat{\boldsymbol{x}}_T)\leq\epsilon$. Therefore, $\hat{\boldsymbol{x}}_T$ is the ϵ-accurate solution.

A.3 Proof of Theorem 4.2

In this subsection, we prove Theorem 4.2. First, we show several lemmas.

Lemma A.4. *For any $t\geq 1$, $\hat{\Pi}_t$ has at least one element (i.e., $\hat{\Pi}_t\neq\emptyset$).*

Proof. Let $t\geq 1$. We define $\tilde{\boldsymbol{x}}_t$ and $\boldsymbol{x}_t^\dagger$ as

$$\begin{aligned}\tilde{\boldsymbol{x}}_t&=\arg\max_{\boldsymbol{x}\in\mathcal{X}}l_t^{(F_2)}(\boldsymbol{x}),\\\boldsymbol{x}_t^\dagger&=\arg\max_{\boldsymbol{x}\in\mathcal{X};l_t^{(F_2)}(\boldsymbol{x})=l_t^{(F_2)}(\tilde{\boldsymbol{x}}_t)}l_t^{(F_1)}(\boldsymbol{x}).\end{aligned}$$

Assume that $E_{t,\boldsymbol{x}_t^\dagger}^{(\mathrm{pes})}=\emptyset$. Then, it holds that

$$\forall\boldsymbol{x}'\in\emptyset=E_{t,\boldsymbol{x}_t^\dagger}^{(\mathrm{pes})},\ \boldsymbol{F}_t^{(\mathrm{pes})}(\boldsymbol{x}_t^\dagger)\not\preceq\boldsymbol{F}_t^{(\mathrm{pes})}(\boldsymbol{x}').$$

This implies that $\boldsymbol{x}_t^\dagger\in\hat{\Pi}_t$.

On the other hand, if $E_{t,\boldsymbol{x}_t^\dagger}^{(\mathrm{pes})}\neq\emptyset$, then the following holds for any $\boldsymbol{x}'\in E_{t,\boldsymbol{x}_t^\dagger}^{(\mathrm{pes})}$:

$$l_t^{(F_2)}(\boldsymbol{x}_t^\dagger)=l_t^{(F_2)}(\tilde{\boldsymbol{x}}_t)\geq l_t^{(F_2)}(\boldsymbol{x}').$$

Here, if $l_t^{(F_2)}(\boldsymbol{x}_t^\dagger) > l_t^{(F_2)}(\boldsymbol{x}')$, it holds that $\boldsymbol{F}_t^{(\mathrm{pes})}(\boldsymbol{x}_t^\dagger) \not\preceq \boldsymbol{F}_t^{(\mathrm{pes})}(\boldsymbol{x}')$. Similarly, if $l_t^{(F_2)}(\boldsymbol{x}_t^\dagger) = l_t^{(F_2)}(\boldsymbol{x}')$, it holds that

$$l_t^{(F_1)}(\boldsymbol{x}_t^\dagger) \geq l_t^{(F_1)}(\boldsymbol{x}').$$

Noting that $\boldsymbol{F}_t^{(\mathrm{pes})}(\boldsymbol{x}_t^\dagger) \neq \boldsymbol{F}_t^{(\mathrm{pes})}(\boldsymbol{x}')$ and $l_t^{(F_2)}(\boldsymbol{x}_t^\dagger) = l_t^{(F_2)}(\boldsymbol{x}')$, we have $l_t^{(F_1)}(\boldsymbol{x}_t^\dagger) > l_t^{(F_1)}(\boldsymbol{x}')$. Thus, we have $\boldsymbol{F}_t^{(\mathrm{pes})}(\boldsymbol{x}_t^\dagger) \not\preceq \boldsymbol{F}_t^{(\mathrm{pes})}(\boldsymbol{x}')$. Form the definition of $\hat{\Pi}_t$, we get $\boldsymbol{x}_t^\dagger \in \hat{\Pi}_t$. ■

Lemma A.5. *Let $t \geq 1$, and assume that $M_t \neq \emptyset$. Also let $\boldsymbol{x}^{(1)}$ be an element of M_t. Then, there exists an element $\boldsymbol{x}' \in \hat{\Pi}_t$ such that*

$$\boldsymbol{F}_t^{(pes)}(\boldsymbol{x}^{(1)}) \preceq \boldsymbol{F}_t^{(pes)}(\boldsymbol{x}').$$

Proof. Let $t \geq 1$, $M_t \neq \emptyset$ and $\boldsymbol{x}^{(1)} \in M_t$. Assume that the following holds:

$$\boldsymbol{F}_t^{(\mathrm{pes})}(\boldsymbol{x}^{(1)}) \not\preceq \boldsymbol{F}_t^{(\mathrm{pes})}(\boldsymbol{x}'),\ \forall \boldsymbol{x}' \in \hat{\Pi}_t. \tag{25}$$

From the definition of M_t, we have $\boldsymbol{x}^{(1)} \notin \hat{\Pi}_t$. Here, since $\boldsymbol{x}^{(1)} \notin \hat{\Pi}_t$, there exists $\boldsymbol{x}^{(2)} \in E_{t,\boldsymbol{x}^{(1)}}^{(\mathrm{pes})}$ such that

$$\boldsymbol{F}_t^{(\mathrm{pes})}(\boldsymbol{x}^{(1)}) \preceq \boldsymbol{F}_t^{(\mathrm{pes})}(\boldsymbol{x}^{(2)}).$$

Therefore, there exists $\boldsymbol{x}^{(3)} \in E_{t,\boldsymbol{x}^{(2)}}^{(\mathrm{pes})}$ such that

$$\boldsymbol{F}_t^{(\mathrm{pes})}(\boldsymbol{x}^{(2)}) \preceq \boldsymbol{F}_t^{(\mathrm{pes})}(\boldsymbol{x}^{(3)}).$$

Furthermore, by combining

$$\boldsymbol{F}_t^{(\mathrm{pes})}(\boldsymbol{x}^{(1)}) \preceq \boldsymbol{F}_t^{(\mathrm{pes})}(\boldsymbol{x}^{(2)}),\ \boldsymbol{F}_t^{(\mathrm{pes})}(\boldsymbol{x}^{(2)}) \preceq \boldsymbol{F}_t^{(\mathrm{pes})}(\boldsymbol{x}^{(3)})$$

we get $\boldsymbol{F}_t^{(\mathrm{pes})}(\boldsymbol{x}^{(1)}) \preceq \boldsymbol{F}_t^{(\mathrm{pes})}(\boldsymbol{x}^{(3)})$. Thus, from (25) we obtain $\boldsymbol{x}^{(3)} \notin \hat{\Pi}_t$. By repeating the same argument, we have $\boldsymbol{x}^{(1)}, \ldots, \boldsymbol{x}^{(|\mathcal{X}|)}$, where $\boldsymbol{x}^{(k)} \notin \hat{\Pi}_t$, $k = 1, \ldots, |\mathcal{X}|$. Next, we show that $\boldsymbol{x}^{(i)} \neq \boldsymbol{x}^{(j)}$ for any i and j with $i \neq j$. In fact, if there exist i and j with $i < j$ such that $\boldsymbol{x}^{(i)} = \boldsymbol{x}^{(j)}$, we get $\boldsymbol{F}_t^{(\mathrm{pes})}(\boldsymbol{x}^{(i)}) = \boldsymbol{F}_t^{(\mathrm{pes})}(\boldsymbol{x}^{(j)})$. Here, from $i \leq j-1$, noting that the definition of $\boldsymbol{x}^{(i)}$ and $\boldsymbol{x}^{(j-1)}$ we get

$$\boldsymbol{F}_t^{(\mathrm{pes})}(\boldsymbol{x}^{(j)}) = \boldsymbol{F}_t^{(\mathrm{pes})}(\boldsymbol{x}^{(i)}) \leq \boldsymbol{F}_t^{(\mathrm{pes})}(\boldsymbol{x}^{(j-1)}).$$

Similarly, from the definition of $\boldsymbol{x}^{(j-1)}$ and $\boldsymbol{x}^{(j)}$, we obtain

$$\boldsymbol{F}_t^{(\mathrm{pes})}(\boldsymbol{x}^{(j-1)}) \leq \boldsymbol{F}_t^{(\mathrm{pes})}(\boldsymbol{x}^{(j)}).$$

Thus, we get $\boldsymbol{F}_t^{(\mathrm{pes})}(\boldsymbol{x}^{(j-1)}) = \boldsymbol{F}_t^{(\mathrm{pes})}(\boldsymbol{x}^{(j)})$. However, it contradicts $\boldsymbol{x}^{(j)} \in E_{t,\boldsymbol{x}^{(j-1)}}^{(\mathrm{pes})}$. Hence, it holds that $\boldsymbol{x}^{(i)} \neq \boldsymbol{x}^{(j)}$ for any i and j with $i \neq j$. Therefore, the set $\{\boldsymbol{x}^{(1)}, \ldots, \boldsymbol{x}^{(|\mathcal{X}|)}\}$ is equal to $\mathcal{X}$. Recall that $\boldsymbol{x}^{(k)} \notin \hat{\Pi}_t$ for any $k = 1, \ldots, |\mathcal{X}|$. By combining this and $\{\boldsymbol{x}^{(1)}, \ldots, \boldsymbol{x}^{(|\mathcal{X}|)}\} = \mathcal{X}$, we have $\hat{\Pi}_t = \emptyset$. However, it contradicts Lemma A.4. Hence, the assumption (25) is incorrect. ■

Lemma A.6. *Let $\boldsymbol{x}$ be an element of $\mathcal{X}$, and let $\boldsymbol{\epsilon} = (\epsilon_1, \epsilon_2)$ be a positive vector. Assume that at least one of the following inequalities holds for any $\boldsymbol{x}' \in \mathcal{X}$:*

$$F_1(\boldsymbol{x}) + \epsilon_1 \geq F_1(\boldsymbol{x}'),\ F_2(\boldsymbol{x}) + \epsilon_2 \geq F_2(\boldsymbol{x}').$$

Then, it holds that $\boldsymbol{F}(\boldsymbol{x}) \in Z_{\boldsymbol{\epsilon}}$.

Proof. In order to prove Lemma A.6, we consider the following two cases:

(1) For any $\boldsymbol{x}, \boldsymbol{x}' \in \Pi$, $\boldsymbol{F}(\boldsymbol{x}) = \boldsymbol{F}(\boldsymbol{x}')$.

(2) There exist $\boldsymbol{x}, \boldsymbol{x}' \in \Pi$ such that $\boldsymbol{F}(\boldsymbol{x}) \neq \boldsymbol{F}(\boldsymbol{x}')$.

First, we consider (1). We define $\boldsymbol{x}^{(1)}$ and $\boldsymbol{x}^{(2)}$ as

$$\tilde{\boldsymbol{x}} = \arg\max_{\boldsymbol{x} \in \mathcal{X}} F_1(\boldsymbol{x}),\ \boldsymbol{x}^{(1)} = \arg\max_{\boldsymbol{x}; F_1(\boldsymbol{x}) = F_1(\tilde{\boldsymbol{x}})} F_2(\boldsymbol{x}),$$
$$\boldsymbol{x}^{\dagger} = \arg\max_{\boldsymbol{x} \in \mathcal{X}} F_2(\boldsymbol{x}),\ \boldsymbol{x}^{(2)} = \arg\max_{\boldsymbol{x}; F_2(\boldsymbol{x}) = F_2(\boldsymbol{x}^{\dagger})} F_1(\boldsymbol{x}).$$

From the definition of $\boldsymbol{x}^{(1)}$ and $\boldsymbol{x}^{(2)}$, it holds that $\boldsymbol{x}^{(1)}, \boldsymbol{x}^{(2)} \in \Pi$. Thus, from (1), we get $\boldsymbol{F}(\boldsymbol{x}^{(1)}) = \boldsymbol{F}(\boldsymbol{x}^{(2)})$. Hence, the following holds for any $\boldsymbol{x}' \in \mathcal{X}$:

$$F_1(\boldsymbol{x}') \leq F_1(\boldsymbol{x}^{(1)}),\ F_2(\boldsymbol{x}') \leq F_2(\boldsymbol{x}^{(2)}) = F_2(\boldsymbol{x}^{(1)}).$$

Therefore, we get $\boldsymbol{F}(\boldsymbol{x}') \preceq \boldsymbol{F}(\boldsymbol{x}^{(1)})$. Note that $\boldsymbol{F}(\boldsymbol{x}^{(1)}) \in Z$. Here, let $\boldsymbol{x} \in \mathcal{X}$. Then, from the lemma's assumption, at least one of the following inequalities holds:

$$F_1(\boldsymbol{x}) + \epsilon_1 \geq F_1(\boldsymbol{x}^{(1)}),\ F_2(\boldsymbol{x}) + \epsilon_2 \geq F_2(\boldsymbol{x}^{(1)}).$$

If $F_1(\boldsymbol{x}) + \epsilon_1 \geq F_1(\boldsymbol{x}^{(1)})$, we set $\boldsymbol{a} = (F_1(\boldsymbol{x}^{(1)}), F_2(\boldsymbol{x}))^\top$. Noting that $F_2(\boldsymbol{x}') \leq F_2(\boldsymbol{x}^{(1)})$ for any $\boldsymbol{x}' \in \mathcal{X}$, we have $\boldsymbol{a} \preceq \boldsymbol{F}(\boldsymbol{x}^{(1)})$. This implies that $\boldsymbol{a} \in Z$. Thus, the following holds:

$$\boldsymbol{a} = (F_1(\boldsymbol{x}^{(1)}), F_2(\boldsymbol{x}))^\top \preceq (F_1(\boldsymbol{x}) + \epsilon_1, F_2(\boldsymbol{x}) + \epsilon_2)^\top = \boldsymbol{F}(\boldsymbol{x}) + \boldsymbol{\epsilon}.$$

Furthermore, since $\boldsymbol{F}(\boldsymbol{x}) \preceq \boldsymbol{F}(\boldsymbol{x}^{(1)})$ and $\boldsymbol{F}(\boldsymbol{x}^{(1)}) \in Z$, we obtain $\boldsymbol{F}(\boldsymbol{x}) \in Z_{\boldsymbol{\epsilon}}$. Similarly, if $F_2(\boldsymbol{x}) + \epsilon_2 \geq F_2(\boldsymbol{x}^{(1)})$, we set $\boldsymbol{b} = (F_1(\boldsymbol{x}), F_2(\boldsymbol{x}^{(1)}))^\top$. Also in this case, by using the same argument, we get $\boldsymbol{b} \in Z$ and

$$\boldsymbol{b} \preceq \boldsymbol{F}(\boldsymbol{x}) + \boldsymbol{\epsilon}.$$

By combining this and $\boldsymbol{F}(\boldsymbol{x}) \preceq \boldsymbol{F}(\boldsymbol{x}^{(1)})$ (and $\boldsymbol{F}(\boldsymbol{x}^{(1)}) \in Z$), we obtain $\boldsymbol{F}(\boldsymbol{x}) \in Z_{\boldsymbol{\epsilon}}$.

Next, we consider (2). From (2), there exist $\boldsymbol{x}^{(1)}, \ldots, \boldsymbol{x}^{(l)}$ such that

$$\boldsymbol{F}(\Pi) = \{\boldsymbol{F}(\boldsymbol{x}) \mid \boldsymbol{x} \in \Pi\} = \{\boldsymbol{F}(\boldsymbol{x}^{(i)}) \mid i = 1, \ldots, l\}, \quad \boldsymbol{F}(\boldsymbol{x}^{(i)}) \neq \boldsymbol{F}(\boldsymbol{x}^{(j)}), i \neq j.$$

Here, without loss of generality, we may assume the following:

$$F_1(\boldsymbol{x}^{(1)}) < \cdots < F_1(\boldsymbol{x}^{(l)}), \quad F_2(\boldsymbol{x}^{(1)}) > \cdots > F_2(\boldsymbol{x}^{(l)}).$$

Let $\boldsymbol{x}$ be an element of $\mathcal{X}$. Assume that there exists j such that

$$F_1(\boldsymbol{x}) + \epsilon_1 \geq F_1(\boldsymbol{x}^{(j)}),\ F_2(\boldsymbol{x}) + \epsilon_2 \geq F_2(\boldsymbol{x}^{(j+1)}).$$

Note that $(F_1(\boldsymbol{x}^{(j)}), F_2(\boldsymbol{x}^{(j+1)})^\top \in Z$. In addition, there exists $i \in \{1, \ldots, l\}$ such that $\boldsymbol{F}(\boldsymbol{x}) \preceq \boldsymbol{F}(\boldsymbol{x}^{(i)}) \in Z$. Therefore, $\boldsymbol{F}(\boldsymbol{x}) \in Z_{\boldsymbol{\epsilon}}$.

Similarly, assume that at least one of the following inequalities holds for any j:

$$F_1(\boldsymbol{x}) + \epsilon_1 < F_1(\boldsymbol{x}^{(j)}),\ F_2(\boldsymbol{x}) + \epsilon_2 < F_2(\boldsymbol{x}^{(j+1)}). \tag{26}$$

Here, if $F_1(\boldsymbol{x}) + \epsilon_1 < F_1(\boldsymbol{x}^{(1)})$, from lemma's assumption it holds that $F_2(\boldsymbol{x}) + \epsilon_2 \geq F_2(\boldsymbol{x}^{(1)})$. Moreover, we define $\boldsymbol{c} = (F_1(\boldsymbol{x}), F_2(\boldsymbol{x}^{(1)}))^\top \in Z$. Then, the following holds:

$$\boldsymbol{F}(\boldsymbol{x}) + \boldsymbol{\epsilon} = (F_1(\boldsymbol{x}) + \epsilon_1, F_2(\boldsymbol{x}) + \epsilon_2)^\top \succeq (F_1(\boldsymbol{x}), F_2(\boldsymbol{x}^{(1)}))^\top = \boldsymbol{c} \in Z.$$

Furthermore, from the definition of $\boldsymbol{x}^{(1)}$, it holds that $F_2(\boldsymbol{x}^{(1)}) \geq F_2(\boldsymbol{x})$. Thus, noting that $F_1(\boldsymbol{x}) + \epsilon_1 < F_1(\boldsymbol{x}^{(1)})$, we get $F_1(\boldsymbol{x}) \leq F_1(\boldsymbol{x}^{(1)})$. By combining these, we have $\boldsymbol{F}(\boldsymbol{x}) \preceq \boldsymbol{F}(\boldsymbol{x}^{(1)}) \in Z$. This implies that $\boldsymbol{F}(\boldsymbol{x}) \in Z_{\boldsymbol{\epsilon}}$. On the other hand, if $F_1(\boldsymbol{x}) + \epsilon_1 \geq F_1(\boldsymbol{x}^{(1)})$, from (26) we get $F_2(\boldsymbol{x}) + \epsilon_2 < F_2(\boldsymbol{x}^{(2)})$. Therefore, from lemma's assumption, we obtain $F_1(\boldsymbol{x}) + \epsilon_1 \geq F_1(\boldsymbol{x}^{(2)})$. By using (26) again, we have $F_2(\boldsymbol{x}) + \epsilon_2 < F_2(\boldsymbol{x}^{(3)})$. Hence, by repeating these procedures, we get $F_1(\boldsymbol{x}) + \epsilon_1 \geq F_1(\boldsymbol{x}^{(l)})$ and $F_2(\boldsymbol{x}) + \epsilon_2 < F_2(\boldsymbol{x}^{(l)})$. Finally, noting that

$$\boldsymbol{F}(\boldsymbol{x}) \preceq (F_1(\boldsymbol{x}^{(l)}), F_2(\boldsymbol{x}) + \epsilon_2)^\top \preceq (F_1(\boldsymbol{x}^{(l)}), F_2(\boldsymbol{x}^{(l)}))^\top = \boldsymbol{F}(\boldsymbol{x}^{(l)}) \in Z,$$
$$\boldsymbol{F}(\boldsymbol{x}) + \boldsymbol{\epsilon} \succeq (F_1(\boldsymbol{x}^{(l)}), F_2(\boldsymbol{x}))^\top \in Z,$$

we get $\boldsymbol{F}(\boldsymbol{x}) \in Z_{\boldsymbol{\epsilon}}$. ■

By using these lemmas, we prove Theorem 4.2.

Proof. First, we prove that the algorithm terminates after at most t' iterations where t' is the positive integer satisfying $\max_{\boldsymbol{x}\in M_{t'}\cup\hat{\Pi}_{t'}} \lambda_{t'}(\boldsymbol{x}) = \lambda_{t'}(\boldsymbol{x}_{t'}) \leq \min\{\epsilon_1, \epsilon_2\}$. From the definition of λ_t, noting that $u_t^{(F_1)}(\boldsymbol{x}) - l_t^{(F_1)}(\boldsymbol{x}) \leq \lambda_t(\boldsymbol{x})$ and $u_t^{(F_2)}(\boldsymbol{x}) - l_t^{(F_2)}(\boldsymbol{x}) \leq \lambda_t(\boldsymbol{x})$, we have

$$\max_{\boldsymbol{x}\in M_{t'}\cup\hat{\Pi}_{t'}} \left\{ u_{t'}^{(F_1)}(\boldsymbol{x}) - l_{t'}^{(F_1)}(\boldsymbol{x}) \right\} \leq \epsilon_1$$

and

$$\max_{\boldsymbol{x}\in M_{t'}\cup\hat{\Pi}_{t'}} \left\{ u_{t'}^{(F_2)}(\boldsymbol{x}) - l_{t'}^{(F_2)}(\boldsymbol{x}) \right\} \leq \epsilon_2.$$

Then, for any $\boldsymbol{x}' \in \hat{\Pi}_t$, it holds that

$$u_{t'}^{(F_1)}(\boldsymbol{x}') \leq l_{t'}^{(F_1)}(\boldsymbol{x}') + \epsilon_1 \tag{27}$$

and

$$u_{t'}^{(F_2)}(\boldsymbol{x}') \leq l_{t'}^{(F_2)}(\boldsymbol{x}') + \epsilon_2. \tag{28}$$

Here, let $\boldsymbol{x}$ be an element of $\hat{\Pi}_{t'}$. Then, from the definition of $\hat{\Pi}_t$, for any $\boldsymbol{x}' \in \hat{\Pi}_{t'}$, at least one of the following inequalities holds:

$$l_{t'}^{(F_1)}(\boldsymbol{x}') \leq l_{t'}^{(F_1)}(\boldsymbol{x}),\ l_{t'}^{(F_2)}(\boldsymbol{x}') \leq l_{t'}^{(F_2)}(\boldsymbol{x}).$$

Thus, from (27) and (28), for any $\boldsymbol{x}' \in \hat{\Pi}_{t'}$, it holds that $\boldsymbol{F}_t^{(\mathrm{pes})}(\boldsymbol{x}) + \boldsymbol{\epsilon} \not\prec \boldsymbol{F}_{t'}^{(\mathrm{opt})}(\boldsymbol{x}')$. This implies that $U_{t'} = \emptyset$. Similarly, if $M_{t'} \neq \emptyset$, there exists $\boldsymbol{x} \in M_{t'}$ such that $\boldsymbol{F}_{t'}^{(\mathrm{opt})}(\boldsymbol{x}) \not\preceq_{\boldsymbol{\epsilon}} \boldsymbol{F}_{t'}^{(\mathrm{pes})}(\boldsymbol{x}')$ for any $\boldsymbol{x}' \in \hat{\Pi}_t$. On the other hand, from Lemma A.5, there exists $\boldsymbol{x}'' \in \hat{\Pi}_{t'}$ such that $\boldsymbol{F}_{t'}^{(\mathrm{pes})}(\boldsymbol{x}) \preceq \boldsymbol{F}_{t'}^{(\mathrm{pes})}(\boldsymbol{x}'')$. Moreover, from (27) and (28), $\boldsymbol{x}''$ satisfies $\boldsymbol{F}_{t'}^{(\mathrm{opt})}(\boldsymbol{x}) \preceq_{\boldsymbol{\epsilon}} \boldsymbol{F}_{t'}^{(\mathrm{pes})}(\boldsymbol{x}'')$. However, it contradicts the definition of M_t. Hence, we get $M_{t'} = \emptyset$.

Hereafter, we assume that (10), (19) and (20) hold. From the definition of λ_t, we obtain

$$\lambda_t(\boldsymbol{x}) \leq \left\{ u_t^{(F_1)}(\boldsymbol{x}) - l_t^{(F_1)}(\boldsymbol{x}) \right\} + \left\{ u_t^{(F_2)}(\boldsymbol{x}) - l_t^{(F_2)}(\boldsymbol{x}) \right\}.$$

This implies that

$$\sum_{t=1}^{T} \lambda_t(\boldsymbol{x}_t) \leq \sum_{t=1}^{T} \left\{ u_t^{(F_1)}(\boldsymbol{x}_t) - l_t^{(F_1)}(\boldsymbol{x}_t) \right\} + \sum_{t=1}^{T} \left\{ u_t^{(F_2)}(\boldsymbol{x}_t) - l_t^{(F_2)}(\boldsymbol{x}_t) \right\}.$$

Therefore, from (12), (18), (19) and (20), we get

$$\begin{aligned}\sum_{t=1}^{T} \lambda_t(\boldsymbol{x}_t) &\leq 4\beta_T^{1/2} \left\{ \sum_{t=1}^{T} \sigma_{t-1}(\boldsymbol{x}_t, \boldsymbol{w}_t) + 4\ln\frac{18}{\delta} \right\} \\ &+ \sqrt{16T\tilde{B}\beta_T^{1/2} \left\{ \sum_{t=1}^{T} \sigma_{t-1}(\boldsymbol{x}_t, \boldsymbol{w}_t) + 4\ln\frac{18}{\delta} \right\} + 40T\beta_T \left\{ \sum_{t=1}^{T} \sigma_{t-1}^2(\boldsymbol{x}_t, \boldsymbol{w}_t) + 4\ln\frac{18}{\delta} \right\}}.\end{aligned}$$

Hence, from (21) and (22), it holds that

$$\frac{1}{T}\sum_{t=1}^{T} \lambda_t(\boldsymbol{x}_t) \leq T^{-1}\beta_T^{1/2} \left\{ \sqrt{2TC_1\gamma_T} + C_2 \right\} + T^{-1}\sqrt{2T\tilde{B}\beta_T^{1/2} \left\{ \sqrt{8TC_1\gamma_T} + 2C_2 \right\} + 5T\beta_T \left\{ C_1\gamma_T + 2C_2 \right\}}. \tag{29}$$

Here, let T be a positive integer such that the right hand side in (29) is less than or equal to $\min\{\epsilon_1, \epsilon_2\}$. Then, there exists a positive integer t' such that $t' \leq T$ and $\lambda_{t'}(\boldsymbol{x}_{t'}) \leq \min\{\epsilon_1, \epsilon_2\}$. Therefore, we have $M_{t'} = \emptyset$ and $U_{t'} = \emptyset$. This means that the algorithm terminates after at most t' iterations.

Next, under (10) we show that $\hat{\Pi}_t$ is the $\boldsymbol{\epsilon}$-accurate Pareto set when $M_t = \emptyset$ and $U_t = \emptyset$. First, we prove $\boldsymbol{F}(\hat{\Pi}_t) \subset Z_{\boldsymbol{\epsilon}}$. Let $\boldsymbol{x}$ be an element of $\hat{\Pi}_t$. For any $\boldsymbol{x}' \in \hat{\Pi}_t \setminus \{\boldsymbol{x}\}$, it holds that $\boldsymbol{F}_t^{(\mathrm{pes})}(\boldsymbol{x}) + \boldsymbol{\epsilon} \not\prec \boldsymbol{F}_t^{(\mathrm{opt})}(\boldsymbol{x}')$ because $U_t = \emptyset$. Furthermore, noting that $M_t = \emptyset$, for any $\boldsymbol{x}' \in \mathcal{X} \setminus \hat{\Pi}_t$, there exists $\boldsymbol{x}'' \in \hat{\Pi}_t$ such that

$\boldsymbol{F}_t^{(\mathrm{opt})}(\boldsymbol{x}') \preceq_{\boldsymbol{\epsilon}} \boldsymbol{F}_t^{(\mathrm{pes})}(\boldsymbol{x}'')$. In addition, since $\boldsymbol{x} \in \hat{\Pi}_t$, from the definition of $\hat{\Pi}_t$, at least one of the following inequalities holds:

$$l_t^{(F_1)}(\boldsymbol{x}'') \leq l_t^{(F_1)}(\boldsymbol{x}), l_t^{(F_2)}(\boldsymbol{x}'') \leq l_t^{(F_2)}(\boldsymbol{x}).$$

By combining this and $\boldsymbol{F}_t^{(\mathrm{opt})}(\boldsymbol{x}') \preceq_{\boldsymbol{\epsilon}} \boldsymbol{F}_t^{(\mathrm{pes})}(\boldsymbol{x}'')$, we get $\boldsymbol{F}_t^{(\mathrm{pes})}(\boldsymbol{x}) + \boldsymbol{\epsilon} \not\preceq \boldsymbol{F}_t^{(\mathrm{opt})}(\boldsymbol{x}')$. Therefore, under (10) at least one of the following inequalities holds for any $\boldsymbol{x}' \in \mathcal{X} \setminus \{\boldsymbol{x}\}$:

$$F_1(\boldsymbol{x}) + \epsilon_1 \geq F_1(\boldsymbol{x}'),\ F_2(\boldsymbol{x}) + \epsilon_2 \geq F_2(\boldsymbol{x}').$$

Moreover, it is clear that $F_1(\boldsymbol{x}) + \epsilon_1 \geq F_1(\boldsymbol{x})$. Hence, from Lemma A.6, we get $\boldsymbol{F}(\hat{\Pi}_t) \subset Z_{\boldsymbol{\epsilon}}$.

Finally, we show that for any $\boldsymbol{x}' \in \Pi$, there exists $\boldsymbol{x} \in \hat{\Pi}_t$ such that $\boldsymbol{x}' \preceq_{\boldsymbol{\epsilon}} \boldsymbol{x}$. When $\boldsymbol{x}' \in \hat{\Pi}_t$, the existence of $\boldsymbol{x}$ is obvious because $\boldsymbol{x}' \preceq_{\boldsymbol{\epsilon}} \boldsymbol{x}'$. On the other hand, when $\boldsymbol{x}' \in \mathcal{X} \setminus \hat{\Pi}_t$, since $M_t = \emptyset$ there exists $\boldsymbol{x} \in \hat{\Pi}_t$ such that $\boldsymbol{F}_t^{(\mathrm{opt})}(\boldsymbol{x}') \preceq_{\boldsymbol{\epsilon}} \boldsymbol{F}_t^{(\mathrm{pes})}(\boldsymbol{x})$. Thus, under (10), this implies that $\boldsymbol{x}' \preceq_{\boldsymbol{\epsilon}} \boldsymbol{x}$. Hence, for any $\boldsymbol{x}' \in \Pi$, there exists $\boldsymbol{x} \in \hat{\Pi}_t$ such that $\boldsymbol{x}' \preceq_{\boldsymbol{\epsilon}} \boldsymbol{x}$. From this and $\boldsymbol{F}(\hat{\Pi}_t) \subset Z_{\boldsymbol{\epsilon}}$, we have that $\hat{\Pi}_t$ is the $\boldsymbol{\epsilon}$-accurate Pareto set. Here, note that (10), (19) and (20) hold with probability at least $1 - \delta$. Therefore, we get the desired result. ■

A.4 Proof of Theorem 4.3

Proof. Assume that (10), (19) and (20) hold. Then, by using the same argument as in the proof of Theorem 4.2, we get

$$\frac{1}{T}\sum_{t=1}^{T} \lambda_t(\boldsymbol{x}_t) \leq T^{-1}\beta_T^{1/2}\left\{\sqrt{2TC_1\gamma_T} + C_2\right\} + T^{-1}\sqrt{2T\tilde{B}\beta_T^{1/2}\left\{\sqrt{8TC_1\gamma_T} + 2C_2\right\} + 5T\beta_T\left\{C_1\gamma_T + 2C_2\right\}}. \tag{30}$$

Here, from the definition of T, the right-hand side of (30) is less than or equal to $\min\{\epsilon_1, \epsilon_2\}$. Hence, there exists a positive integer $t' \leq T$ such that $\max_{\boldsymbol{x} \in M_{t'}} \lambda_{t'}(\boldsymbol{x}) = \lambda_{t'}(\boldsymbol{x}_{t'}) \leq \min\{\epsilon_1, \epsilon_2\}$. This implies that the algorithm terminates after at most T iterations.

Next, we prove claim 2 of the theorem. Assume that $\boldsymbol{x}^*$ exists. Here, we consider the two cases $\boldsymbol{x}^* \in M_{t'}^{(\mathrm{obj})}$ and $\boldsymbol{x}^* \notin M_{t'}^{(\mathrm{obj})}$. For case $\boldsymbol{x}^* \in M_{t'}^{(\mathrm{obj})}$, since (10) holds, the following inequality holds:

$$h - \epsilon_2 \leq h \leq F_2(\boldsymbol{x}^*) \leq u_{t'}^{(F_2)}(\boldsymbol{x}^*).$$

This means that $\boldsymbol{x}^* \in M_{t'}^{(\mathrm{cons})}$. Therefore, we have $\boldsymbol{x}^* \in M_{t'}$. Furthermore, noting that $u_t^{(F_1)}(\boldsymbol{x}) - l_t^{(F_1)}(\boldsymbol{x}) \leq \lambda_t(\boldsymbol{x})$ and $u_t^{(F_2)}(\boldsymbol{x}) - l_t^{(F_2)}(\boldsymbol{x}) \leq \lambda_t(\boldsymbol{x})$, it holds that

$$\max_{\boldsymbol{x} \in M_{t'}} \left\{u_{t'}^{(F_1)}(\boldsymbol{x}) - l_{t'}^{(F_1)}(\boldsymbol{x})\right\} \leq \epsilon_1, \tag{31}$$

$$\max_{\boldsymbol{x} \in M_{t'}} \left\{u_{t'}^{(F_2)}(\boldsymbol{x}) - l_{t'}^{(F_2)}(\boldsymbol{x})\right\} \leq \epsilon_2. \tag{32}$$

Here, if $l_{t'}^{(F_2)}(\boldsymbol{x}^*) < h - \epsilon_2$, then from (32), we get $u_{t'}^{(F_2)}(\boldsymbol{x}^*) < h$. Thus, from (10), we obtain $F_2(\boldsymbol{x}^*) < h$. However, this contradicts the definition of $\boldsymbol{x}^*$, implying that $l_{t'}^{(F_2)}(\boldsymbol{x}^*) \geq h - \epsilon_2$ and $\boldsymbol{x}^* \in S_{t'} \neq \emptyset$. Moreover, from (31) the following holds:

$$\begin{aligned}
&\max_{\boldsymbol{x} \in M_{t'}} \left\{u_{t'}^{(F_1)}(\boldsymbol{x}) - l_{t'}^{(F_1)}(\boldsymbol{x})\right\} \leq \epsilon_1 \\
\Rightarrow &u_{t'}^{(F_1)}(\boldsymbol{x}^*) - l_{t'}^{(F_1)}(\boldsymbol{x}^*) \leq \epsilon_1 \\
\Rightarrow &u_{t'}^{(F_1)}(\boldsymbol{x}^*) - \max_{\boldsymbol{x} \in S_{t'}} l_{t'}^{(F_1)}(\boldsymbol{x}) \leq \epsilon_1 \\
\Rightarrow &u_{t'}^{(F_1)}(\boldsymbol{x}^*) - l_{t'}^{(F_1)}(\hat{\boldsymbol{x}}_{t'}) \leq \epsilon_1 \\
\Rightarrow &l_{t'}^{(F_1)}(\hat{\boldsymbol{x}}_{t'}) \geq u_{t'}^{(F_1)}(\boldsymbol{x}^*) - \epsilon_1.
\end{aligned}$$

In addition, from the definition of $S_{t'}$, we have

$$l_{t'}(\hat{\boldsymbol{x}}_{t'}) \geq h - \epsilon_2.$$

On the other hand, if $\boldsymbol{x}^* \notin M_{t'}^{(\mathrm{obj})}$, then $M_{t'}^{(\mathrm{obj})} \neq \mathcal{X}$. Thus, from the definition of $M_{t'}^{(\mathrm{obj})}$, it holds that $S_{t'} \neq \emptyset$. Therefore, we get

$$l_{t'}(\hat{\boldsymbol{x}}_{t'}) = \max_{\boldsymbol{x} \in S_{t'}} l_{t'}(\boldsymbol{x}) \geq h - \epsilon_2.$$

Furthermore, since $\boldsymbol{x}^* \notin M_{t'}^{(\mathrm{obj})}$, it holds that

$$u_{t'}^{(F_1)}(\boldsymbol{x}^*) - \epsilon_1 \leq u_{t'}^{(F_1)}(\boldsymbol{x}^*) < l_{t'}^{(F_1)}(\hat{\boldsymbol{x}}_{t'}) - \epsilon_1 \leq l_{t'}^{(F_1)}(\hat{\boldsymbol{x}}_{t'}).$$

Therefore, if $\boldsymbol{x}^*$ exists, then we have $S_{t'} \neq \emptyset$ and

$$l_{t'}^{(F_1)}(\hat{\boldsymbol{x}}_{t'}) \geq u_{t'}^{(F_1)}(\boldsymbol{x}^*) - \epsilon_1, \tag{33}$$

$$l_{t'}(\hat{\boldsymbol{x}}_{t'}) \geq h - \epsilon_2. \tag{34}$$

Note that (33) and (34) imply that $\hat{\boldsymbol{x}}_{t'}$ is an ϵ-accurate solution when (10) holds. Finally, since (10), (19) and (20) hold with probability at least $1 - \delta$, we have Theorem 4.3. ■

B Details of Section 3.3

B.1 Noisy Input Setting

In this subsection, we consider the setting where the input $\boldsymbol{x}$ contains a noise $\boldsymbol{\xi} \in \Delta$. Let $\mathcal{X} \subset \mathbb{R}^d$ be an input space for optimization. In addition, assume that $\mathcal{X}$ is a finite set. Furthermore, let $\Delta \subset \mathbb{R}^d$ be a compact and convex set, and let $\boldsymbol{\xi}$ be a random noise satisfying $\boldsymbol{\xi} \in \Delta$. Moreover, let f be a black-box function on $\mathcal{D} \coloneqq \{\boldsymbol{x} + \boldsymbol{\xi} \mid \boldsymbol{x} \in \mathcal{X}, \boldsymbol{\xi} \in \Delta\}$, and let $k : \mathcal{D} \times \mathcal{D} \to \mathbb{R}$ be a positive-definite kernel with $f \in \mathcal{H}_k$ and $\|f\|_{\mathcal{H}_k} \leq B$.

For each step t, we select an observation point $\boldsymbol{x}_t \in \mathcal{X}$, and the observed value is obtained as $y_t = f(\boldsymbol{x}_t + \boldsymbol{\xi}_t) + \eta_t$. Here, η_t is the independent normal distribution $\eta_t \sim \mathcal{N}(0, \sigma^2)$, and $\boldsymbol{\xi}_t$ is the observed value of $\boldsymbol{\xi}$.

In this setting, the expected value and variance of $f(\boldsymbol{x})$ with respect to $\boldsymbol{\xi}$ are given by

$$\mathbb{E}_{\boldsymbol{\xi}}[f(\boldsymbol{x} + \boldsymbol{\xi})] = \int_{\Delta} f(\boldsymbol{x} + \boldsymbol{\xi}) p(\boldsymbol{\xi}) \mathrm{d}\boldsymbol{\xi}, \tag{35}$$

$$\mathbb{V}_{\boldsymbol{\xi}}[f(\boldsymbol{x} + \boldsymbol{\xi})] = \int_{\Delta} \{f(\boldsymbol{x} + \boldsymbol{\xi}) - \mathbb{E}_{\boldsymbol{\xi}}[f(\boldsymbol{x} + \boldsymbol{\xi})]\}^2 p(\boldsymbol{\xi}) \mathrm{d}\boldsymbol{\xi}, \tag{36}$$

where $p(\boldsymbol{\xi})$ is a known probability density function of $\boldsymbol{\xi}$. Similarly as in (3), using (35) and (36) we define the optimization objective functions F_1 and F_2. In addition, let $\mu_t(\boldsymbol{x})$, $\sigma_t^2(\boldsymbol{x})$ and $Q_t(\boldsymbol{x}) \coloneqq [l_t(\boldsymbol{x}), u_t(\boldsymbol{x})]$ denote the posterior mean, posterior variance and confidence bound of $f(\boldsymbol{x})$ at the step t, respectively.

Confidence Bound Confidence bounds of objective functions F_1 and F_2 defined by using (35) and (36) can also be constructed by using the same procedure as in §3.2. First, assume that $f(\tilde{\boldsymbol{x}}) \in Q_t(\tilde{\boldsymbol{x}})$ for any $\tilde{\boldsymbol{x}} \in \mathcal{D}$. Then, the following holds for any $\boldsymbol{x} \in \mathcal{X}$:

$$\int_{\Delta} l_t(\boldsymbol{x} + \boldsymbol{\xi}) p(\boldsymbol{\xi}) \mathrm{d}\boldsymbol{\xi} \leq \int_{\Delta} f(\boldsymbol{x} + \boldsymbol{\xi}) p(\boldsymbol{\xi}) \mathrm{d}\boldsymbol{\xi} \leq \int_{\Delta} u_t(\boldsymbol{x} + \boldsymbol{\xi}) p(\boldsymbol{\xi}) \mathrm{d}\boldsymbol{\xi}.$$

Therefore, the confidence bound $Q_t^{(F_1)}(\boldsymbol{x})$ of $F_1(\boldsymbol{x})$ can be constructed as $Q_t^{(F_1)}(\boldsymbol{x}) \coloneqq [l_t^{(F_1)}(\boldsymbol{x}), u_t^{(F_1)}(\boldsymbol{x})]$ using

$$l_t^{(F_1)}(\boldsymbol{x}) = \int_{\Delta} l_t(\boldsymbol{x} + \boldsymbol{\xi}) p(\boldsymbol{\xi}) \mathrm{d}\boldsymbol{\xi},\ u_t^{(F_1)}(\boldsymbol{x}) = \int_{\Delta} u_t(\boldsymbol{x} + \boldsymbol{\xi}) p(\boldsymbol{\xi}) \mathrm{d}\boldsymbol{\xi}.$$

Similarly, the confidence bound $Q_t^{(F_2)}(\boldsymbol{x})$ of $F_2(\boldsymbol{x})$ can be expressed as $Q_t^{(F_2)}(\boldsymbol{x}) \coloneqq [l_t^{(F_2)}(\boldsymbol{x}), u_t^{(F_2)}(\boldsymbol{x})]$ using

$$l_t^{(F_2)}(\boldsymbol{x}) = -\sqrt{\int_{\Delta} \tilde{u}_t^{(\mathrm{sq})}(\boldsymbol{x} + \boldsymbol{\xi}) p(\boldsymbol{\xi}) \mathrm{d}\boldsymbol{\xi}},\ l_t^{(F_2)}(\boldsymbol{x}) = -\sqrt{\int_{\Delta} \tilde{l}_t^{(\mathrm{sq})}(\boldsymbol{x} + \boldsymbol{\xi}) p(\boldsymbol{\xi}) \mathrm{d}\boldsymbol{\xi}},$$

where $\tilde{l}_t^{(\mathrm{sq})}(\boldsymbol{x}+\boldsymbol{\xi})$ and $\tilde{u}_t^{(\mathrm{sq})}(\boldsymbol{x}+\boldsymbol{\xi})$ are given by

$$\tilde{l}_t(\boldsymbol{x}+\boldsymbol{\xi}) = l_t(\boldsymbol{x}+\boldsymbol{\xi}) - \mathbb{E}_{\boldsymbol{\xi}}[u_t(\boldsymbol{x}+\boldsymbol{\xi})],$$
$$\tilde{u}_t(\boldsymbol{x}+\boldsymbol{\xi}) = u_t(\boldsymbol{x}+\boldsymbol{\xi}) - \mathbb{E}_{\boldsymbol{\xi}}[l_t(\boldsymbol{x}+\boldsymbol{\xi})],$$
$$\tilde{l}_t^{(\mathrm{sq})}(\boldsymbol{x}+\boldsymbol{\xi}) = \begin{cases} 0 & \text{if } \tilde{l}_t(\boldsymbol{x}+\boldsymbol{\xi}) \le 0 \le \tilde{u}_t(\boldsymbol{x}+\boldsymbol{\xi}), \\ \min\left\{\tilde{l}_t^2(\boldsymbol{x}+\boldsymbol{\xi}), \tilde{u}_t^2(\boldsymbol{x}+\boldsymbol{\xi})\right\} & \text{otherwise} \end{cases},$$
$$\tilde{u}_t^{(\mathrm{sq})}(\boldsymbol{x}+\boldsymbol{\xi}) = \max\left\{\tilde{l}_t^2(\boldsymbol{x}+\boldsymbol{\xi}), \tilde{u}_t^2(\boldsymbol{x}+\boldsymbol{\xi})\right\}.$$

Using $Q_t^{(F_1)}$ and $Q_t^{(F_2)}$ above, we can construct the proposed algorithm in the same procedure.

B.2 Simulator Based Experiment

In this subsection, we consider the setting that $\boldsymbol{w}_t$ can be selected in the optimization phase at each step. Furthermore, we show theoretical guarantees in this setting. Hereafter, we only discuss the multi-task scenario, but the same argument can be made for multi-objective and constraint optimization scenarios by selecting $\boldsymbol{w}_t$ and $\boldsymbol{\xi}_t$ in the same procedure.

In our proposed algorithm, $(\boldsymbol{x}_t, \boldsymbol{w}_t)$ at the step t is selected by

$$\boldsymbol{x}_t = \arg\max_{\boldsymbol{x}\in\mathcal{X}} u_t^{(G)}(\boldsymbol{x}),$$
$$\boldsymbol{w}_t = \arg\max_{\boldsymbol{w}\in\Omega} \sigma_{t-1}(\boldsymbol{x}_t, \boldsymbol{w}).$$

In this algorithm, the following theorem holds:

Theorem B.1. *Let k be a positive-definite kernel, and let $f \in \mathcal{H}_k$ with $\|f\|_{\mathcal{H}_k} \le B$. Also let $\delta \in (0,1)$, $\epsilon > 0$, and define $\beta_t = \left(\sqrt{2(\gamma_{t-1} + \ln(1/\delta))} + B\right)^2$. Moreover, for any t, define $\hat{\boldsymbol{x}}_t = \mathrm{argmax}_{\boldsymbol{x}_{t'} \in \{\boldsymbol{x}_1,\ldots,\boldsymbol{x}_t\}} l_{t'}^{(G)}(\boldsymbol{x}_{t'})$. Then, when the proposed algorithm in the simulator based setting is performed, $\hat{\boldsymbol{x}}_T$ is the ϵ-accurate solution with probability at least $1-\delta$, where T is the smallest positive integer satisfying*

$$\alpha T^{-1} \beta_T^{1/2} \sqrt{TC_1\gamma_T} + (1-\alpha)T^{-1}\sqrt{4T\tilde{B}\beta_T^{1/2}\sqrt{TC_1\gamma_T} + 5T\beta_T C_1 \gamma_T} \le \epsilon.$$

Here, $\tilde{B}$ and C_1 are given by $\tilde{B} = \max_{(\boldsymbol{x},\boldsymbol{w})\in(\mathcal{X}\times\Omega)} \{f(\boldsymbol{x},\boldsymbol{w}) - \mathbb{E}_{\boldsymbol{w}}[f(\boldsymbol{x},\boldsymbol{w})]\}$ and $C_1 = \frac{8}{\ln(1+\sigma^{-2})}$.

Proof. Assume that (10) holds. Then, from Lemma A.1 we have

$$\sum_{t=1}^T \left\{u_t^{(G)}(\boldsymbol{x}_t) - l_t^{(G)}(\boldsymbol{x}_t)\right\} \le 2\alpha\beta_T^{1/2} \sum_{t=1}^T \int_\Omega \sigma_{t-1}(\boldsymbol{x}_t, \boldsymbol{w}) p(\boldsymbol{w}) \mathrm{d}\boldsymbol{w}$$
$$+ (1-\alpha)\sqrt{8T\tilde{B}\beta_T^{1/2} \sum_{t=1}^T \int_\Omega \sigma_{t-1}(\boldsymbol{x}_t, \boldsymbol{w}) p(\boldsymbol{w}) \mathrm{d}\boldsymbol{w} + 20T\beta_T \sum_{t=1}^T \int_\Omega \sigma_{t-1}^2(\boldsymbol{x}_t, \boldsymbol{w}) p(\boldsymbol{w}) \mathrm{d}\boldsymbol{w}}.$$

In addition, from the definition of $\boldsymbol{w}_t$, it holds that

$$\sum_{t=1}^T \int_\Omega \sigma_{t-1}(\boldsymbol{x}_t, \boldsymbol{w}) p(\boldsymbol{w}) \mathrm{d}\boldsymbol{w} \le \sum_{t=1}^T \sigma_{t-1}(\boldsymbol{x}_t, \boldsymbol{w}_t),$$
$$\sum_{t=1}^T \int_\Omega \sigma_{t-1}^2(\boldsymbol{x}_t, \boldsymbol{w}) p(\boldsymbol{w}) \mathrm{d}\boldsymbol{w} \le \sum_{t=1}^T \sigma_{t-1}^2(\boldsymbol{x}_t, \boldsymbol{w}_t).$$

Hence, we get

$$\sum_{t=1}^T \left\{u_t^{(G)}(\boldsymbol{x}_t) - l_t^{(G)}(\boldsymbol{x}_t)\right\} \le 2\alpha\beta_T^{1/2} \sum_{t=1}^T \sigma_{t-1}(\boldsymbol{x}_t, \boldsymbol{w}_t) + (1-\alpha)\sqrt{8T\tilde{B}\beta_T^{1/2} \sum_{t=1}^T \sigma_{t-1}(\boldsymbol{x}_t, \boldsymbol{w}_t) + 20T\beta_T \sum_{t=1}^T \sigma_{t-1}^2(\boldsymbol{x}_t, \boldsymbol{w}_t)}.$$

Furthermore, from (21) and (22), we obtain

$$\sum_{t=1}^{T} \left\{ u_t^{(G)}(\boldsymbol{x}_t) - l_t^{(G)}(\boldsymbol{x}_t) \right\} \leq \alpha \beta_T^{1/2} \sqrt{C_1 T \gamma_T} + (1-\alpha) \sqrt{4T\tilde{B}\beta_T^{1/2}\sqrt{C_1 T \gamma_T} + 5T\beta_T C_1 \gamma_T}.$$

Finally, by using the same argument as in the proof of Theorem 4.1, the following inequality holds:

$$G(\boldsymbol{x}^*) - G(\hat{\boldsymbol{x}}_T) \leq \sum_{t=1}^{T} \left\{ u_t^{(G)}(\boldsymbol{x}_t) - l_t^{(G)}(\boldsymbol{x}_t) \right\} / T.$$

Therefore, noting that the definition of T, we get the desired result. ■

Noisy Input Extension Here, we extend the setting defined in subsection 3.3.1to the simulator based setting. Since there is the noise $\boldsymbol{\xi} \in \Delta$ instead of $\boldsymbol{w}$, we consider the observation point $\boldsymbol{x}_t$ at the step t as $\boldsymbol{x}_t := \tilde{\boldsymbol{x}}_t + \boldsymbol{\xi}_t$, where $(\tilde{\boldsymbol{x}}_t, \boldsymbol{\xi}_t)$ is given by

$$\begin{aligned} \tilde{\boldsymbol{x}}_t &= \arg\max_{\boldsymbol{x} \in \mathcal{X}} u_t^{(G)}(\boldsymbol{x}), \\ \boldsymbol{\xi}_t &= \arg\max_{\boldsymbol{\xi} \in \Delta} \sigma_{t-1}(\tilde{\boldsymbol{x}}_t + \boldsymbol{\xi}). \end{aligned}$$

Then, similar theorems as in Theorem B.1 hold. However, the practical performance of this algorithm is not much different from that of Uncertainty Sampling, which was used as the base method in numerical experiments. For this reason, in the simulator based noisy input setting, we propose a method for selecting $(\tilde{\boldsymbol{x}}_t, \boldsymbol{\xi}_t)$ as follows:

$$\begin{aligned} \tilde{\boldsymbol{x}}_t &= \arg\max_{\boldsymbol{x} \in \mathcal{X}} u_t^{(G)}(\boldsymbol{x}), \\ \boldsymbol{\xi}_t &= \arg\max_{\boldsymbol{\xi} \in \Delta} \sigma_{t-1}(\tilde{\boldsymbol{x}}_t + \boldsymbol{\xi}) p(\boldsymbol{\xi}). \end{aligned}$$

In order to derive similar convergence results as in Theorem B.1, we assume that the probability density function $p(\boldsymbol{\xi})$ of $\boldsymbol{\xi}$ is a bounded function on Δ, i.e., $\sup_{\boldsymbol{\xi} \in \mathcal{D}} p(\boldsymbol{\xi}) < \infty$.

Theorem B.2. *Let $\delta \in (0,1)$, $\epsilon > 0$, and set $\beta_t = \left(\sqrt{2(\gamma_{t-1} + \ln(1/\delta))} + B \right)^2$. For any t, define $\hat{\boldsymbol{x}}_t = \mathrm{argmax}_{\boldsymbol{x}_{t'} \in \{\boldsymbol{x}_1, \ldots, \boldsymbol{x}_t\}} l_{t'}^{(G)}(\boldsymbol{x}_{t'})$. Moreover, assume that $\sup_{\boldsymbol{\xi} \in \Delta} p(\boldsymbol{\xi}) \leq R < \infty$. Then, when the proposed algorithm in the simulator based noisy input setting is performed, $\hat{\boldsymbol{x}}_T$ is the ϵ-accurate solution with probability at least $1-\delta$, where T is the smallest positive integer satisfying*

$$\alpha T^{-1} \beta_T^{1/2} R \sqrt{T C_1 \gamma_T} + (1-\alpha) T^{-1} \sqrt{4T\tilde{B}R\beta_T^{1/2}\sqrt{TC_1\gamma_T} + 5TR\beta_T C_1 \gamma_T} \leq \epsilon.$$

Here, $\tilde{B}$ and C_1 are given by $\tilde{B} = \max_{(\boldsymbol{x}, \boldsymbol{\xi}) \in (\mathcal{X} \times \Delta)} \{ f(\boldsymbol{x} + \boldsymbol{\xi}) - \mathbb{E}_{\boldsymbol{\xi}}[f(\boldsymbol{x} + \boldsymbol{\xi})] \}$ and $C_1 = \frac{8}{\ln(1+\sigma^{-2})}$.

Proof. Similarly as in Lemma A.1, with probability at least $1-\delta$, it holds that

$$\begin{aligned} \sum_{t=1}^{T} \left\{ u_t^{(G)}(\boldsymbol{x}_t) - l_t^{(G)}(\boldsymbol{x}_t) \right\} &\leq 2\alpha\beta_T^{1/2} \sum_{t=1}^{T} \int_{\Delta} \sigma_{t-1}(\boldsymbol{x}_t + \boldsymbol{\xi}) p(\boldsymbol{\xi}) \mathrm{d}\boldsymbol{\xi} \\ &+ (1-\alpha) \sqrt{8T\tilde{B}\beta_T^{1/2} \sum_{t=1}^{T} \int_{\Delta} \sigma_{t-1}(\boldsymbol{x}_t + \boldsymbol{\xi}) p(\boldsymbol{w}) \mathrm{d}\boldsymbol{\xi} + 20T\beta_T \sum_{t=1}^{T} \int_{\Delta} \sigma_{t-1}^2(\boldsymbol{x}_t + \boldsymbol{\xi}) p(\boldsymbol{\xi}) \mathrm{d}\boldsymbol{\xi}}. \end{aligned}$$

Moreover, from the definition of $\boldsymbol{\xi}_t$, we have

$$\begin{aligned} \sum_{t=1}^{T} \int_{\Delta} \sigma_{t-1}(\boldsymbol{x}_t + \boldsymbol{\xi}) p(\boldsymbol{\xi}) \mathrm{d}\boldsymbol{\xi} &\leq \sum_{t=1}^{T} \sigma_{t-1}(\boldsymbol{x}_t + \boldsymbol{\xi}_t) p(\boldsymbol{\xi}_t) \leq R \sum_{t=1}^{T} \sigma_{t-1}(\boldsymbol{x}_t + \boldsymbol{\xi}_t), \\ \sum_{t=1}^{T} \int_{\Omega} \sigma_{t-1}^2(\boldsymbol{x}_t + \boldsymbol{\xi}) p(\boldsymbol{\xi}) \mathrm{d}\boldsymbol{\xi} &\leq \sum_{t=1}^{T} \sigma_{t-1}^2(\boldsymbol{x}_t + \boldsymbol{\xi}_t) p(\boldsymbol{\xi}_t) \leq R \sum_{t=1}^{T} \sigma_{t-1}^2(\boldsymbol{x}_t + \boldsymbol{\xi}_t). \end{aligned}$$

Thus, we get

$$\sum_{t=1}^{T}\left\{u_t^{(G)}(\boldsymbol{x}_t)-l_t^{(G)}(\boldsymbol{x}_t)\right\}\leq 2\alpha\beta_T^{1/2}R\sum_{t=1}^{T}\sigma_{t-1}(\boldsymbol{x}_t+\boldsymbol{\xi}_t)+(1-\alpha)\sqrt{8T\tilde{B}\beta_T^{1/2}R\sum_{t=1}^{T}\sigma_{t-1}(\boldsymbol{x}_t+\boldsymbol{\xi}_t)+20T\beta_T R\sum_{t=1}^{T}\sigma_{t-1}^2(\boldsymbol{x}_t+\boldsymbol{\xi}_t)},$$

and

$$\sum_{t=1}^{T}\left\{u_t^{(G)}(\boldsymbol{x}_t)-l_t^{(G)}(\boldsymbol{x}_t)\right\}\leq \alpha\beta_T^{1/2}R\sqrt{C_1T\gamma_T}+(1-\alpha)\sqrt{4T\tilde{B}R\beta_T^{1/2}\sqrt{C_1T\gamma_T}+5T\beta_T RC_1\gamma_T}.$$

By using the same argument as in the proof of 4.1, we obtain the following inequality:

$$G(\boldsymbol{x}^*)-G(\hat{\boldsymbol{x}}_T)\leq\sum_{t=1}^{T}\left\{u_t^{(G)}(\boldsymbol{x}_t)-l_t^{(G)}(\boldsymbol{x}_t)\right\}/T.$$

Therefore, we get the desired result. ■

C Extension to Continuous Set

In this section, we consider the setting where $\mathcal{X}$ is a continuous set. First, in MT-MVA-BO, $\boldsymbol{x}_t = \mathrm{argmax}_{\boldsymbol{x}\in\mathcal{X}} u_t^{(G)}(\boldsymbol{x})$ can be calculated by using a continuous optimization solver. However, in MO-MVA-BO, it is difficult to calculate the estimated Pareto set $\hat{\Pi}_t$ and set of latent optimal solutions M_t. In this paper, based on Srinivas et al. (2010) we extend the proposed algorithm by using a discretization set $\tilde{\mathcal{X}}$ of $\mathcal{X}$.

Hereafter, let $\mathcal{X}=[0,1]^{d_1}$. Furthermore, assume that f is an L-Lipschitz continuous function, i.e., there exists $L>0$ such that

$$|f(\boldsymbol{x},\boldsymbol{w})-f(\boldsymbol{x}',\boldsymbol{w})|\leq L\|\boldsymbol{x}-\boldsymbol{x}'\|_1,$$

for any $\boldsymbol{x},\boldsymbol{x}'\in\mathcal{X}$. Note that Lipschitz continuity holds if standard kernels are used (Sui et al., 2015, 2018).

From Lipschitz continuity of f, the following lemmas about F_1 and F_2 hold:

Lemma C.1. *Let f be an L-Lipschitz continuous function. Then, it holds that*

$$|F_1(\boldsymbol{x})-F_1(\boldsymbol{x}')|\leq L\|\boldsymbol{x}-\boldsymbol{x}'\|_1,\ \forall\boldsymbol{x},\boldsymbol{x}'\in\mathcal{X},$$

where F_1 is given by (3).

Proof. From the definition of F_1 and Lipschitz continuity of f, the following inequality holds:

$$\begin{aligned}|F_1(\boldsymbol{x})-F_1(\boldsymbol{x}')| &= \left|\int_\Omega\{f(\boldsymbol{x},\boldsymbol{w})-f(\boldsymbol{x}',\boldsymbol{w})\}p(\boldsymbol{w})\mathrm{d}\boldsymbol{w}\right|\\ &\leq\int_\Omega|f(\boldsymbol{x},\boldsymbol{w})-f(\boldsymbol{x}',\boldsymbol{w})|p(\boldsymbol{w})\mathrm{d}\boldsymbol{w}\\ &\leq L\|\boldsymbol{x}-\boldsymbol{x}'\|_1.\end{aligned}$$

■

Lemma C.2. *Let f be an L-Lipschitz continuous function, $\tilde{B}=\max_{(\boldsymbol{x},\boldsymbol{w})\in(\mathcal{X}\times\Omega)}|f(\boldsymbol{x},\boldsymbol{w})-\mathbb{E}_{\boldsymbol{w}}[f(\boldsymbol{x},\boldsymbol{w})]|$, and define F_2 as in (3). Then, the following inequality holds for any $\boldsymbol{x},\boldsymbol{x}'\in\mathcal{X}$:*

$$|F_2(\boldsymbol{x})-F_2(\boldsymbol{x}')|\leq\sqrt{4\tilde{B}L\|\boldsymbol{x}-\boldsymbol{x}'\|_1}.$$

Proof. From Lipschitz continuity of f, for any $\boldsymbol{x},\boldsymbol{x}'\in\mathcal{X}$, $\boldsymbol{w}\in\Omega$, it holds that

$$\begin{aligned}&\left|\{f(\boldsymbol{x},\boldsymbol{w})-\mathbb{E}_{\boldsymbol{w}}[f(\boldsymbol{x},\boldsymbol{w})]\}^2-\{f(\boldsymbol{x}',\boldsymbol{w})-\mathbb{E}_{\boldsymbol{w}}[f(\boldsymbol{x}',\boldsymbol{w})]\}^2\right|\\ =&|\{f(\boldsymbol{x},\boldsymbol{w})-\mathbb{E}_{\boldsymbol{w}}[f(\boldsymbol{x},\boldsymbol{w})]\}-\{f(\boldsymbol{x}',\boldsymbol{w})-\mathbb{E}_{\boldsymbol{w}}[f(\boldsymbol{x}',\boldsymbol{w})]\}|\times|\{f(\boldsymbol{x},\boldsymbol{w})-\mathbb{E}_{\boldsymbol{w}}[f(\boldsymbol{x},\boldsymbol{w})]\}+\{f(\boldsymbol{x}',\boldsymbol{w})-\mathbb{E}_{\boldsymbol{w}}[f(\boldsymbol{x}',\boldsymbol{w})]\}|\\ \leq&(|f(\boldsymbol{x},\boldsymbol{w})-f(\boldsymbol{x}',\boldsymbol{w})|+|\mathbb{E}_{\boldsymbol{w}}[f(\boldsymbol{x},\boldsymbol{w})]-\mathbb{E}_{\boldsymbol{w}}[f(\boldsymbol{x}',\boldsymbol{w})]|)\times(|f(\boldsymbol{x},\boldsymbol{w})-\mathbb{E}_{\boldsymbol{w}}[f(\boldsymbol{x},\boldsymbol{w})]|+|f(\boldsymbol{x}',\boldsymbol{w})-\mathbb{E}_{\boldsymbol{w}}[f(\boldsymbol{x}',\boldsymbol{w})]|)\\ \leq&2L\|\boldsymbol{x}-\boldsymbol{x}'\|_1\times 2\tilde{B}\\ =&4\tilde{B}L\|\boldsymbol{x}-\boldsymbol{x}'\|_1.\end{aligned}$$

Here, if $F_2(\boldsymbol{x}) \geq F_2(\boldsymbol{x}')$, then

$$
\begin{aligned}
&|F_2(\boldsymbol{x}) - F_2(\boldsymbol{x}')| \\
=&F_2(\boldsymbol{x}) - F_2(\boldsymbol{x}') \\
=&\sqrt{\int_\Omega \left\{f(\boldsymbol{x}', \boldsymbol{w}) - \mathbb{E}_{\boldsymbol{w}}[f(\boldsymbol{x}', \boldsymbol{w})]\right\}^2 p(\boldsymbol{w}) \mathrm{d}\boldsymbol{w}} - \sqrt{\int_\Omega \left\{f(\boldsymbol{x}, \boldsymbol{w}) - \mathbb{E}_{\boldsymbol{w}}[f(\boldsymbol{x}, \boldsymbol{w})]\right\}^2 p(\boldsymbol{w}) \mathrm{d}\boldsymbol{w}} \\
\leq&\sqrt{\int_\Omega \left\{f(\boldsymbol{x}', \boldsymbol{w}) - \mathbb{E}_{\boldsymbol{w}}[f(\boldsymbol{x}', \boldsymbol{w})]\right\}^2 p(\boldsymbol{w}) \mathrm{d}\boldsymbol{w} - \int_\Omega \left\{f(\boldsymbol{x}, \boldsymbol{w}) - \mathbb{E}_{\boldsymbol{w}}[f(\boldsymbol{x}, \boldsymbol{w})]\right\}^2 p(\boldsymbol{w}) \mathrm{d}\boldsymbol{w}} \\
\leq&\sqrt{\int_\Omega \left| \left\{f(\boldsymbol{x}', \boldsymbol{w}) - \mathbb{E}_{\boldsymbol{w}}[f(\boldsymbol{x}', \boldsymbol{w})]\right\}^2 - \left\{f(\boldsymbol{x}, \boldsymbol{w}) - \mathbb{E}_{\boldsymbol{w}}[f(\boldsymbol{x}, \boldsymbol{w})]\right\}^2 \right| p(\boldsymbol{w}) \mathrm{d}\boldsymbol{w}} \\
\leq&\sqrt{4\tilde{B}L\|\boldsymbol{x} - \boldsymbol{x}'\|_1}.
\end{aligned}
$$

On the other hand, if $F_2(\boldsymbol{x}) < F_2(\boldsymbol{x}')$, it holds that $|F_2(\boldsymbol{x}) - F_2(\boldsymbol{x}')| \leq \sqrt{4\tilde{B}L\|\boldsymbol{x} - \boldsymbol{x}'\|_1}$. Therefore, for any $\boldsymbol{x}, \boldsymbol{x}' \in \mathcal{X}$, the desired inequality holds. ■

Moreover, the following lemma holds:

Lemma C.3. *Let Z be the Pareto front for $\mathcal{X}$, and let $\boldsymbol{\epsilon} = (\epsilon_1, \epsilon_2)^\top$ be a positive vector. Define*

$$
\begin{aligned}
Z^+ &= \bigcup_{(y_1, y_2) \in Z} (-\infty, y_1] \times (-\infty, y_2],\ Z^-(\boldsymbol{\epsilon}) = \bigcup_{(y_1, y_2) \in Z} (-\infty, y_1 - \epsilon_1) \times (-\infty, y_2 - \epsilon_2), \\
Z^*(\boldsymbol{\epsilon}) &= \{(y_1 - \epsilon_1', y_2 - \epsilon_2') \mid (y_1, y_2) \in Z,\ 0 \leq \epsilon_1' \leq \epsilon_1, 0 \leq \epsilon_2' \leq \epsilon_2\}.
\end{aligned}
$$

Then, it holds that

$$
Z^+ = Z^-(\boldsymbol{\epsilon}) \cup Z^*(\boldsymbol{\epsilon}),\ Z^-(\boldsymbol{\epsilon}) \cap Z^*(\boldsymbol{\epsilon}) = \emptyset.
$$

Proof. First, we show $Z^-(\boldsymbol{\epsilon}) \cap Z^*(\boldsymbol{\epsilon}) = \emptyset$. Let $\boldsymbol{y}$ be an element of $Z^-(\boldsymbol{\epsilon})$. Then, there exists $(y_1', y_2') \in Z$ such that

$$
y_1 < y_1' - \epsilon_1,\ y_2 < y_2' - \epsilon_2.
$$

Here, for any $(y_1'', y_2'') \in Z$, y_1'' satisfies $y_1' \leq y_1''$ or $y_1' > y_1''$. If $y_1' \leq y_1''$, from $y_1 < y_1' - \epsilon_1$ we get

$$
\boldsymbol{y} \notin \{(y_1'' - \epsilon_1', y_2'' - \epsilon_2') \mid 0 \leq \epsilon_1' \leq \epsilon_1, 0 \leq \epsilon_2' \leq \epsilon_2\}.
$$

On the other hand, if $y_1' > y_1''$, then y_2'' satisfies $y_2' \leq y_2''$ because the inequality $y_2' > y_2''$ implies that $(y_1'', y_2'') \in (-\infty, y_1') \times (-\infty, y_2')$. However, it contradicts that $(y_1'', y_2'') \in Z$. From $y_2' \leq y_2''$ and $y_2 < y_2' - \epsilon_2$, we have

$$
\boldsymbol{y} \notin \{(y_1'' - \epsilon_1', y_2'' - \epsilon_2') \mid 0 \leq \epsilon_1' \leq \epsilon_1, 0 \leq \epsilon_2' \leq \epsilon_2\}.
$$

Therefore, it holds that $\boldsymbol{y} \notin Z^*(\boldsymbol{\epsilon})$. This implies that $Z^-(\boldsymbol{\epsilon}) \cap Z^*(\boldsymbol{\epsilon}) = \emptyset$.

Next, we show $Z^+ = Z^-(\boldsymbol{\epsilon}) \cup Z^*(\boldsymbol{\epsilon})$. It is clear that $Z^+ \supset Z^-(\boldsymbol{\epsilon}) \cup Z^*(\boldsymbol{\epsilon})$. Thus, we only show that $Z^+ \subset Z^-(\boldsymbol{\epsilon}) \cup Z^*(\boldsymbol{\epsilon})$. Let $\boldsymbol{y}$ be an element of Z^+. If $\boldsymbol{y} \in Z^-(\boldsymbol{\epsilon})$, it holds that $\boldsymbol{y} \in Z^-(\boldsymbol{\epsilon}) \cup Z^*(\boldsymbol{\epsilon})$. On the other hand, if $\boldsymbol{y} \notin Z^-(\boldsymbol{\epsilon})$, at least one of the following inequalities holds for any $(y_1', y_2') \in Z$:

$$
y_1 \geq y_1' - \epsilon_1,\ y_2 \geq y_2' - \epsilon_2.
$$

If there exists $\epsilon_1' \in [0, \epsilon_1]$ such that $(y_1 + \epsilon_1', y_2) \in Z$, then $\boldsymbol{y} \in Z^*(\boldsymbol{\epsilon})$. Next, we consider the case that $(y_1 + \epsilon_1', y_2) \notin Z$ for any $\epsilon_1' \in [0, \epsilon_1]$. Let $Z' = \{\boldsymbol{a} = (a_1, a_2) \in Z \mid y_1 \leq a_1 \leq y + \epsilon_1\}$. Here, assume that $y_2 < a_2 - \epsilon_2$ for any $\boldsymbol{a} \in Z'$. Then, from continuity of Z, there exists $\hat{\boldsymbol{y}} = (\hat{y}_1, \hat{y}_2) \in Z$ such that $y_1 < \hat{y}_1 - \epsilon_1$ and $y_2 < \hat{y}_2 - \epsilon_2$. However, it contradicts $\boldsymbol{y} \notin Z^-(\boldsymbol{\epsilon})$. Hence, there exists an element $\boldsymbol{a} = (a_1, a_2) \in Z'$ such that $y_2 \geq a_2 - \epsilon_2$. Moreover, there exists $b \geq y_2$ such that $(y_1, b) \in Z$. This implies that there exist $\tilde{\epsilon}_1$ and $\tilde{\epsilon}_2$ such that $0 \leq \tilde{\epsilon}_1 \leq \epsilon_1$, $0 \leq \tilde{\epsilon}_2 \leq \epsilon_2$ and $(y_1 + \tilde{\epsilon}_1, y_2 + \tilde{\epsilon}_2) \in Z$. Therefore, it holds that $\boldsymbol{y} \in Z^*(\boldsymbol{\epsilon})$. ■

Next, we explain the method of constructing $\tilde{\mathcal{X}}$. Let $\tilde{\mathcal{X}}$ be a set of grid points when each dimension of $\mathcal{X} = [0,1]^{d_1}$ is divided into τ evenly spaced segments. Also let $[\boldsymbol{x}] \in \tilde{\mathcal{X}}$ be a point closest to $\boldsymbol{x} \in \mathcal{X}$ with respect to the $L1$-distance. Then, it holds that

$$\|\boldsymbol{x} - [\boldsymbol{x}]\|_1 \leq \frac{d_1}{\tau}, \ \forall \boldsymbol{x} \in \mathcal{X}. \tag{37}$$

In the proposed algorithm for the continuous set setting, Algorithm 1 is performed by using $\tilde{\mathcal{X}}$ instead of $\mathcal{X}$. Then, we define the estimated Pareto set $\hat{\Pi}_t$, latent Pareto set M_t and uncertain set U_t in Algorithm 1 as

$$\begin{aligned}
\hat{\Pi}_t &= \left\{ \boldsymbol{x} \in \tilde{\mathcal{X}} \mid \forall \boldsymbol{x}' \in \tilde{E}^{(\mathrm{pes})}_{t,\boldsymbol{x}}, \ \boldsymbol{F}^{(\mathrm{pes})}_t(\boldsymbol{x}) \not\preceq \boldsymbol{F}^{(\mathrm{pes})}_t(\boldsymbol{x}') \right\}, \ \tilde{E}^{(\mathrm{pes})}_{t,\boldsymbol{x}} = \{\boldsymbol{x}' \in \tilde{\mathcal{X}} \mid \boldsymbol{F}^{(\mathrm{pes})}_t(\boldsymbol{x}) \neq \boldsymbol{F}^{(\mathrm{pes})}_t(\boldsymbol{x}')\}, \\
M_t &= \left\{ \boldsymbol{x} \in \tilde{\mathcal{X}} \setminus \hat{\Pi}_t \mid \forall \boldsymbol{x}' \in \hat{\Pi}_t, \ \boldsymbol{F}^{(\mathrm{opt})}_t(\boldsymbol{x}) \not\preceq_{\boldsymbol{\epsilon}/2} \boldsymbol{F}^{(\mathrm{pes})}_t(\boldsymbol{x}') \right\}, \\
U_t &= \left\{ \boldsymbol{x} \in \hat{\Pi}_t \mid \exists \boldsymbol{x}' \in \hat{\Pi}_t \setminus \{\boldsymbol{x}\}, \boldsymbol{F}^{(\mathrm{pes})}_t(\boldsymbol{x}) + \boldsymbol{\epsilon}/2 \prec \boldsymbol{F}^{(\mathrm{opt})}_t(\boldsymbol{x}') \right\}.
\end{aligned}$$

Note that $\boldsymbol{\epsilon}/2$, not $\boldsymbol{\epsilon}$ is used to calculate $\tilde{M}_t$ and $\tilde{U}_t$.

In the algorithm using $\tilde{\mathcal{X}}$, the following theorem holds:

Theorem C.1. *Let $\tilde{B} = \max_{(\boldsymbol{x},\boldsymbol{w}) \in (\mathcal{X} \times \Omega)} |f(\boldsymbol{x},\boldsymbol{w}) - \mathbb{E}_{\boldsymbol{w}}[f(\boldsymbol{x},\boldsymbol{w})]|$, and let $\delta \in (0,1)$, $\boldsymbol{\epsilon} = (\epsilon_1, \epsilon_2)$ where $\epsilon_1 > 0$ and $\epsilon_2 > 0$. Define $\beta_t = \left(\sqrt{2(\gamma_{t-1} + \ln(3/\delta))} + B\right)^2$ and $\tau = \max\left\{\frac{2Ld_1}{\epsilon_1}, \frac{16\tilde{B}Ld_1}{\epsilon_2^2}\right\}$. Then, the following (1) and (2) hold with probability at least $1-\delta$:*

(1) *The algorithm terminates after at most T iterations, where T is the smallest positive integer satisfying*

$$T^{-1}\beta_T^{1/2}\left(\sqrt{2TC_1\gamma_T} + C_2\right) + T^{-1}\sqrt{2T\tilde{B}\beta_T^{1/2}\left(\sqrt{8TC_1\gamma_T} + 2C_2\right) + 5T\beta_T\left(C_1\gamma_T + 2C_2\right)} \leq \min\{\epsilon_1, \epsilon_2\}/2.$$

Here, C_1 and $C2$ are given by $C_1 = \frac{16}{\ln(1+\sigma^{-2})}$ and $C_2 = 16\ln\frac{18}{\delta}$.

(2) *When the algorithm is terminated, the estimated Pareto set $\hat{\Pi}$ is the ϵ-accurate Pareto Set.*

Proof. We omit the proof of (1) because its proof is the same as in the proof of Theorem 4.2. We only prove (2). From (37) and Lemma C.1–C.2, the following holds for any $\boldsymbol{x} \in \mathcal{X}$:

$$\begin{aligned}
|F_1(\boldsymbol{x}) - F_1([\boldsymbol{x}])| &\leq L\|\boldsymbol{x} - [\boldsymbol{x}]\|_1 \\
&= \frac{\epsilon_1}{2}, \qquad (38) \\
|F_2(\boldsymbol{x}) - F_2([\boldsymbol{x}])| &\leq \sqrt{4\tilde{B}L\|\boldsymbol{x} - [\boldsymbol{x}]\|_1} \\
&= \frac{\epsilon_2}{2}. \qquad (39)
\end{aligned}$$

Assume that (10) holds. Let $\tilde{Z}$ be a Pareto front for $\tilde{\mathcal{X}}$. Then, for any $\boldsymbol{y} \in \tilde{Z}$, it holds that

$$\boldsymbol{y} \in \bigcup_{(y_1', y_2') \in Z} (-\infty, y_1'] \times (-\infty, y_2'], \tag{40}$$

where Z is the Pareto front for $\mathcal{X}$. Similarly, let

$$Z^-(\boldsymbol{\epsilon}/2) = \bigcup_{(y_1', y_2') \in Z} (-\infty, y_1' - \epsilon_1/2) \times (-\infty, y_2' - \epsilon_2/2).$$

Then, for any $\boldsymbol{y}'' \in Z^-(\boldsymbol{\epsilon}/2)$, there exists $\boldsymbol{x} \in \mathcal{X}$ such that

$$y_1'' < F_1(\boldsymbol{x}) - \epsilon_1/2, \ y_2'' < F_2(\boldsymbol{x}) - \epsilon_2/2.$$

Here, from (38) and (39) we have

$$F_1(\boldsymbol{x}) \leq F_1([\boldsymbol{x}]) + \epsilon_1/2, F_2(\boldsymbol{x}) \leq F_2([\boldsymbol{x}]) + \epsilon_2/2.$$

Algorithm 1 Multi-objective MVA-BO (MO-MVA-BO)

Input: GP prior $\mathcal{GP}(0,\ k)$, $\{\beta_t\}_{t\in\mathbb{N}}$, Non-negative vector $\boldsymbol{\epsilon} = (\epsilon_1, \epsilon_2)$.
  $t \leftarrow 0$.
  repeat
    Compute $\hat{\Pi}_t, M_t$.
    Compute $\lambda_t(\boldsymbol{x})$ for any $\boldsymbol{x} \in M_t \cup \hat{\Pi}_t$.
    Choose $\boldsymbol{x}_t = \mathrm{argmax}_{\boldsymbol{x}\in M_t \cup \hat{\Pi}_t} \lambda_t(\boldsymbol{x})$.
    Sample $\boldsymbol{w}_t \sim p(\boldsymbol{w})$.
    Observe $y_t \leftarrow f(\boldsymbol{x}_t, \boldsymbol{w}_t) + \eta_t$.
    Update the GP by adding $((\boldsymbol{x}_t, \boldsymbol{w}_t), y_t)$.
    $t \leftarrow t + 1$.
    Compute U_t.
  until $M_t = \emptyset$ and $U_t = \emptyset$
Output: $\hat{\Pi}_t$.

Thus, it holds that $y_1'' < F_1([\boldsymbol{x}])$ and $y_2'' < F_2([\boldsymbol{x}])$. This implies that

$$Z^-(\boldsymbol{\epsilon}/2) \subset \{\boldsymbol{y} \in \mathbb{R} \mid \exists \boldsymbol{x} \in \tilde{\mathcal{X}},\ \boldsymbol{y} \preceq \boldsymbol{F}(\boldsymbol{x})\} \equiv A.$$

Here, since $Z^-(\boldsymbol{\epsilon}/2)$ is the open set, noting that $Z^-(\boldsymbol{\epsilon}/2) \subset A$ we get $Z^-(\boldsymbol{\epsilon}/2) \subset \mathrm{int}(A)$, where $\mathrm{int}(A)$ is the interior of A. In addition, from the definition of the interior and boundary (frontier), we obtain $\mathrm{int}(A) \cap \partial A = \emptyset$. Therefore, from $\partial A = \tilde{Z}$ and $Z^-(\boldsymbol{\epsilon}/2) \subset \mathrm{int}(A)$, it holds that $Z^-(\boldsymbol{\epsilon}/2) \cap \tilde{Z} = \emptyset$. Hence, for any $\boldsymbol{y} \in \tilde{Z}$, $\boldsymbol{y} \notin Z^-(\boldsymbol{\epsilon}/2)$. Thus, by using this and (40), from Lemma C.3, it holds that

$$\tilde{Z} \subset Z^*(\boldsymbol{\epsilon}/2).$$

Hence, for any $\boldsymbol{y} \in \tilde{Z}$, there exists $\boldsymbol{a} \in Z$ such that

$$y_1 = a_1 - \epsilon_1', y_2 = a_2 - \epsilon_2', \quad 0 \le \epsilon_1' \le \epsilon_1/2,\ 0 \le \epsilon_2' \le \epsilon_2/2. \tag{41}$$

Furthermore, from Theorem 4.2, for any $\boldsymbol{x} \in \hat{\Pi}_t$, there exists $\boldsymbol{y}^\dagger \in \tilde{Z}$ such that

$$y_1^\dagger \le F_1(\boldsymbol{x}) + \epsilon_1/2,\ y_2^\dagger \le F_2(\boldsymbol{x}) + \epsilon_2/2.$$

By combining this and (41), we get

$$a_1 = y_1^\dagger + \epsilon_1' \le F_1(\boldsymbol{x}) + \epsilon_1/2 + \epsilon_1' \le F_1(\boldsymbol{x}) + \epsilon_1,$$
$$a_2 = y_2^\dagger + \epsilon_2' \le F_2(\boldsymbol{x}) + \epsilon_2/2 + \epsilon_2' \le F_2(\boldsymbol{x}) + \epsilon_2.$$

Therefore, we have $\boldsymbol{F}(\hat{\Pi}_t) \subset Z_{\boldsymbol{\epsilon}}$.

Furthermore, let $\boldsymbol{x} \in \Pi$. For $[x] \in \tilde{\mathcal{X}}$, since $\hat{\Pi}_t$ is the $(\boldsymbol{\epsilon}/2)$-accurate Pareto set for $\tilde{\mathcal{X}}$, there exists $\boldsymbol{x}' \in \hat{\Pi}_t$ such that $\boldsymbol{F}([\boldsymbol{x}]) \preceq_{\boldsymbol{\epsilon}/2} \boldsymbol{F}(\boldsymbol{x}')$. Moreover, form (38) and (39), it holds that $\boldsymbol{F}(\boldsymbol{x}) \le \boldsymbol{F}([\boldsymbol{x}]) + \boldsymbol{\epsilon}/2$. This implies that $\boldsymbol{F}(\boldsymbol{x}) \preceq \boldsymbol{F}([\boldsymbol{x}]) + \boldsymbol{\epsilon}/2 \preceq \boldsymbol{F}(\boldsymbol{x}') + \boldsymbol{\epsilon}$. Therefore, for any $\boldsymbol{x} \in \Pi$, there exits $\boldsymbol{x}' \in \hat{\Pi}_t$ such that $\boldsymbol{x} \preceq_{\boldsymbol{\epsilon}} \boldsymbol{x}'$. Thus, $\hat{\Pi}_t$ is the $\boldsymbol{\epsilon}$-accurate Pareto set for $\mathcal{X}$. ■

D Algorithms and Computational Details

D.1 Pseudo-codes

We show the pseudo-codes of our proposed algorithms corresponding to multi-objective and constraint optimization scenarios in Algorithm 1 and 2, respectively.

D.2 Computation of $l_t^{(F_1)}$, $u_t^{(F_1)}$, $l_t^{(F_2)}$ and $u_t^{(F_2)}$

In the case that Ω is continuous set, $l_t^{(F_1)}$, $u_t^{(F_1)}$, $l_t^{(F_2)}$ and $u_t^{(F_2)}$ depend on the integral of $\boldsymbol{w}$. However, these integrals cannot be computed analytically except for special cases (e.g., in the case that $p(\boldsymbol{w})$ is Normal, and

Algorithm 2 Constrained MVA-BO (Co-MVA-BO)

Input: GP prior $\mathcal{GP}(0,\ k)$, $\{\beta_t\}_{t\in\mathbb{N}}$, Threshold h, Non-negative vector $\boldsymbol{\epsilon} = (\epsilon_1, \epsilon_2)$.
  $M_0 \leftarrow \mathcal{X}$, $S_0 \leftarrow \emptyset$, $t \leftarrow 0$.
  Compute $\lambda_0(\boldsymbol{x})$ for any $\boldsymbol{x} \in M_0$
  while $\max_{\boldsymbol{x}\in M_t} \lambda_t(\boldsymbol{x}) \not\leq \min\{\epsilon_1, \epsilon_2\}$ **do**
    Choose $\boldsymbol{x}_t = \mathrm{argmax}_{\boldsymbol{x}\in M_t} \lambda_t(\boldsymbol{x})$.
    Sample $\boldsymbol{w}_t \sim p(\boldsymbol{w})$.
    Observe $y_t \leftarrow f(\boldsymbol{x}_t, \boldsymbol{w}_t) + \eta_t$.
    Update the GP by adding $((\boldsymbol{x}_t, \boldsymbol{w}_t), y_t)$.
    $t \leftarrow t + 1$.
    Compute S_t, M_t.
    Compute $\lambda_t(\boldsymbol{x})$ for any $\boldsymbol{x} \in M_t$
  end while
  if $S_t \neq \emptyset$ **then**
    Output $\hat{\boldsymbol{x}}_t = \mathrm{argmax}_{\boldsymbol{x}\in S_t} l_t^{(F_1)}(\boldsymbol{x})$.
  end if

k is Gaussian kernel). Thus, we suppose that the user approximate these integrals based on some numerical integration scheme. The computational drawback of the numerical integration is its scalability to the dimension of $\boldsymbol{w}$. In Girard (2004), they computed these types of integrals via polynomial approximation of integrand by Taylor expansion. Their method can be applied for $l_t^{(F_1)}$ and $u_t^{(F_1)}$, but not for $l_t^{(F_2)}$ and $u_t^{(F_2)}$ due to the non-differentiable points of integrands. We leave the efficient computation of $l_t^{(F_2)}$ and $u_t^{(F_2)}$ in the case of high-dimensional $\boldsymbol{w}$ to future works.

D.3 Computational Complexity

Multi-task and Constraint Optimization Scenarios We consider the computational complexity of each one loop of the proposed method in the multi-task and the constrained optimization scenarios. Hereafter, we assume that all integrals of proposed algorithms are computed through the quadrature which leverages M representative points. First, in order to compute $l_t^{(F_1)}(\boldsymbol{x}), u_t^{(F_1)}(\boldsymbol{x}), l_t^{(F_2)}(\boldsymbol{x})$ and $u_t^{(F_2)}(\boldsymbol{x})$ for all $\boldsymbol{x} \in \mathcal{X}$, we need to compute the confidence interval of f at $M|\mathcal{X}|$ representative points. The computation of the confidence bound at one point needs $O(t^2)$, where t represents the current number of steps. (Note that t also represents the number of training samples of the GP.) Therefore, to compute confidence bounds of F_1 and F_2, $O(|\mathcal{X}|Mt^2)$ computations are required. Finally, we need to update the GP posterior at the end of the loop through $O(t^3)$ calculations thus total cost of one loop becomes $O(|\mathcal{X}|Mt^2 + t^3)$.

Multi-objective Optimization Scenario In the multi-objective scenario, to compute $\hat{\Pi}_t$, we need to find the pessimistic Pareto set which is based on $\boldsymbol{F}_t^{(\mathrm{pes})}$. Given the set of finite 2D vectors, an algorithm to identify its Pareto set efficiently is proposed in Kung et al. (1975) and requires $O(|\mathcal{X}|\log|\mathcal{X}|)$ costs. Next, $|\hat{\Pi}_t||\mathcal{X} \setminus \hat{\Pi}_t|$ comparisons are required to compute M_t and U_t. In worst case, this can be $O(|\mathcal{X}|^2)$ costs. However, in practice, this becomes much smaller costs for most loops. Finally, considering the costs to compute confidence bound and the GP posterior update, total cost of one loop becomes $O(|\mathcal{X}|^2 + |\mathcal{X}|Mt^2 + t^3)$.

In our multi-objective scenario, we can modify our MO-MVA-BO to the $\boldsymbol{\epsilon}$-PAL style algorithm (Zuluaga et al., 2016), by considering the intersections of $Q_t^{(F_1)}$ and $Q_t^{(F_2)}$ through every step. This modified version of algorithm can reduce $O(|\mathcal{X}|^2+|\mathcal{X}|Mt^2+t^3)$ to $O(|\mathcal{X}|\log|\mathcal{X}|+|\mathcal{X}|Mt^2+t^3)$ costs. However, in practice, we found intersected confidence bounds sometimes degenerate the algorithm performance especially when the kernel hyperparameters are updated online. For example, we suppose that an erroneous hyperparameter is estimated in one step and a narrower confidence bounds is constructed compared to that of true kernel. Then, the algorithm that takes the intersection is affected by erroneously narrow confidence bound in all the subsequent steps.

Finally, MO-MVA-BO requires a large amount of cost when $\mathcal{X}$ is huge. Especially in the case where $\boldsymbol{x}$ is high-dimensional, the number of elements of $\mathcal{X}$ tends to swell in practice. As discussed in Section 5.5 in Zuluaga et al. (2016), one way to overcome this issue is to consider the extension of the algorithm which is not rely on the discretization of $\mathcal{X}$, and we defer it to future works.

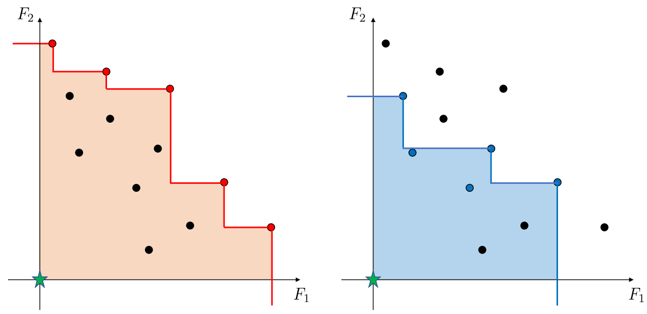

Figure 1: Simple examples of HV and $\hat{\mathrm{HV}}_t$. The red points in the left figure represent the values of F_1 and F_2 at points in Pareto set Π. Given a reference point (green star), hyper volume HV is computed as the area of the region filled in light red. The blue points in the right figure represent the values of F_1 and F_2 at points in estimated Pareto set $\hat{\Pi}_t$, and estimated hyper volume $\hat{\mathrm{HV}}_t$ is computed as the area of the region filled in light blue.

E Additional Experiments

In this section, we show the details of §5 and additional experimental results.

E.1 Implementation Details

Methods for Comparison In our experiments, we used following methods for comparison:

Random Sampling (RS) This method chooses the next point $\boldsymbol{x}_t$ from $\mathcal{X}$ uniformly at random. In the simulator-based setting, $(\boldsymbol{x}_t, \boldsymbol{w}_t)$ is chosen from $\mathcal{X} \times \Omega$ uniformly at random.

Uncertainty Sampling (US) This method defines the next point $\boldsymbol{x}_t$ as $\boldsymbol{x}_t = \mathrm{argmax}_{\boldsymbol{x} \in \mathcal{X}} \int_\Omega \sigma_{t-1}(\boldsymbol{x}, \boldsymbol{w}) p(\boldsymbol{w}) \mathrm{d}\boldsymbol{w}$. In the simulator-based setting, $(\boldsymbol{x}_t, \boldsymbol{w}_t)$ is defined as $(\boldsymbol{x}_t, \boldsymbol{w}_t) = \mathrm{argmax}_{(\boldsymbol{x}, \boldsymbol{w} \in (\mathcal{X} \times \Omega))} \sigma_{t-1}(\boldsymbol{x}, \boldsymbol{w})$.

BQOUCB This method defines next point $\boldsymbol{x}_t$ as $\boldsymbol{x}_t = \mathrm{argmax}_{\boldsymbol{x} \in \mathcal{X}} \mathrm{u}_t^{(F_1)}(\boldsymbol{x})$. In the simulator-based setting, this method chooses $\boldsymbol{w}_t$ as $\boldsymbol{w}_t = \mathrm{argmax}_{\boldsymbol{w} \in \Omega} \sigma_{t-1}(\boldsymbol{x}_t, \boldsymbol{w})$ after the selection of $\boldsymbol{x}_t$.

BO-VO This method defines next point $\boldsymbol{x}_t$ as $\boldsymbol{x}_t = \mathrm{argmax}_{\boldsymbol{x} \in \mathcal{X}} \int_\Omega \mathrm{u}_t^{(F_2)}(\boldsymbol{x}, \boldsymbol{w}) p(\boldsymbol{w}) \mathrm{d}\boldsymbol{w}$. In simulator-based experiments, $\boldsymbol{w}_t$ is chosen in the same way of BQOUCB.

Hyper volume Computation Hyper volume HV is defined as the area between Pareto front and a pre-specified reference point. At every step t, the estimated hyper volume $\hat{\mathrm{HV}}_t$ is computed by using estimated Pareto set $\hat{\Pi}_t$ instead of Pareto set Π. Figure 1 illustrates the example of HV and $\hat{\mathrm{HV}}_t$. In our experiments, we defined reference point as $(\min_{\boldsymbol{x} \in \mathcal{X}} F_1(\boldsymbol{x}), \min_{\boldsymbol{x} \in \mathcal{X}} F_2(\boldsymbol{x}))$, and computed $\mathrm{HV} - \hat{\mathrm{HV}}_t$ as the performance measure.

Constraint Optimization Experiments In constraint optimization experiments, we adopted `RS`, `US`, and `BQOUCB` for comparison. We defined $\hat{\boldsymbol{x}}_t$ as $\hat{\boldsymbol{x}}_t = \mathrm{argmax}_{\boldsymbol{x} \in S_t} l_t^{(F_1)}(\boldsymbol{x})$ in `RS` and `US`, and $\hat{\boldsymbol{x}}_t = \mathrm{argmax}_{\boldsymbol{x} \in \mathcal{X}} l_t^{(F_1)}(\boldsymbol{x})$ in `BQOUCB`. Moreover, we adopted `ADA-BQO-UCB` which is the adaptive version of `BQOUCB`. `ADA-BQO-UCB` chooses next point in the same way of `BQOUCB`, but its $\hat{\boldsymbol{x}}_t$ is defined as $\hat{\boldsymbol{x}}_t = \mathrm{argmax}_{\boldsymbol{x} \in S_t} l_t^{(F_1)}(\boldsymbol{x})$. To measure performances, we used utility gap measure (Hernández-Lobato et al., 2016), which is commonly used as a performance measure in constraint Bayesian optimization problems. At every step t, we reported the following utility gap:

$$\mathrm{UtilityGap}_t = \begin{cases} F_1(\boldsymbol{x}^*) - F_1(\hat{\boldsymbol{x}}_t) & \text{if } F_2(\hat{\boldsymbol{x}}_t) \geq h, \\ F_1(\boldsymbol{x}^*) - \min_{\boldsymbol{x} \in \mathcal{X}} F_1(\boldsymbol{x}) & \text{otherwise} \end{cases},$$

as a performance measure.

Others To make initial points, we combined $2(d_1 + 1)$ randomly selected points from $\mathcal{X}$ with the same number of sample $\boldsymbol{w}$ which is sampled from $p(\boldsymbol{w})$. In simulator-based setting, we chose $2(d_1 + d_2 + 1)$ initial points randomly from $\mathcal{X} \times \Omega$. To compute $Q_t^{(F_1)}$ and $Q_t^{(F_2)}$, we set $\beta_t^{1/2} = 2$ in the multi-task and multi-objective scenarios, and $\beta^{1/2} = 1$ in the constraint optimization scenario because the theoretically recommended values of β_t are well-known to be overly conservative. In §E.2.3, we analyzed the effect of β_t selection experimentally. Furthermore, to simplify experiments, we set $\boldsymbol{\epsilon} = (0, 0)$ and $\epsilon = 0$ in multi-objective and constraint optimization experiments respectively.

E.2 Artificial-data Experiments

E.2.1 GP Test Function

We experimented with test functions of GPs, which are defined by Gaussian kernel and 5/2-Matérn kernel respectively. In 5/2-Matérn kernel experiments, we used $k((\boldsymbol{x}, \boldsymbol{w}), (\boldsymbol{x}', \boldsymbol{w}')) = \sigma_{\mathrm{ker}}^2(1 + \sqrt{5}r + \frac{5}{3}r^2)\exp(-\sqrt{5}r)$, where $r = \sqrt{\|\boldsymbol{x}_j - \boldsymbol{x}_j'\|^2/l^2 + \|\boldsymbol{w}_j - \boldsymbol{w}_j'\|^2/l^2}$ with $l = 0.25$ and $\sigma_{\mathrm{ker}} = 1$. In multi-task optimization scenario, we varied α with $\{0.25, 0.5, 0.75\}$. In constraint optimization scenario, we set $h = -1$. Other settings are the same as section 5.1. Figure 2, 3 and 4 show the experimental results of multi-task, multi-objective, and constraint optimization scenario, respectively. We also conducted experiments in the simulator-based setting. Figure 5, 6 and 7 show the experimental results of multi-task, multi-objective, and constraint optimization scenario in the simulator-based setting, respectively.

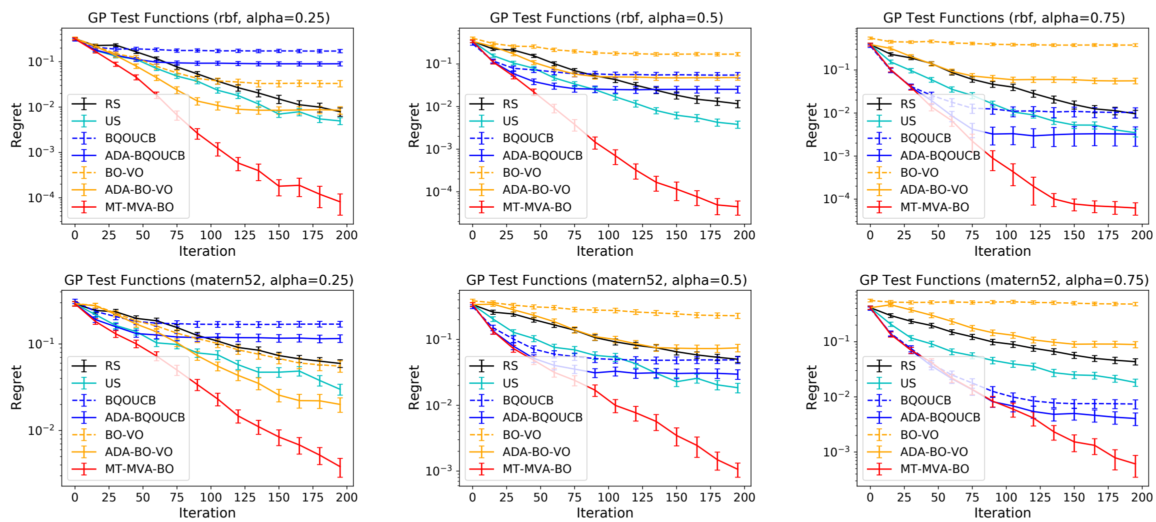

Figure 2: Average performances of multi-task optimization experiments with GP test functions. The top and bottom figures show the results of experiments with Gaussian and 5/2-Matérn kernels, respectively. The left, middle and right figures correspond to the results with $\alpha = 0.25, 0.5$ and 0.75, respectively.

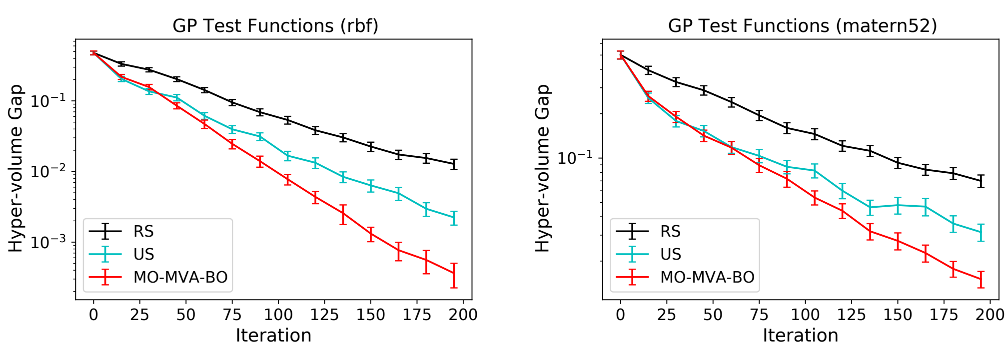

Figure 3: Average performances of multi-objective optimization experiments with GP test functions. The left, and right figures correspond to the results with Gaussian and 5/2-Matérn kernels, respectively.

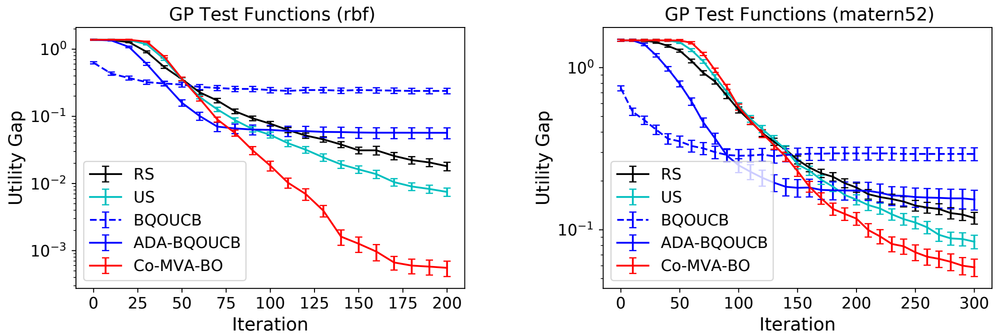

Figure 4: Average performances of constraint optimization experiments with GP test functions. The left, and right figures correspond to the results with Gaussian and 5/2-Matérn kernels, respectively.

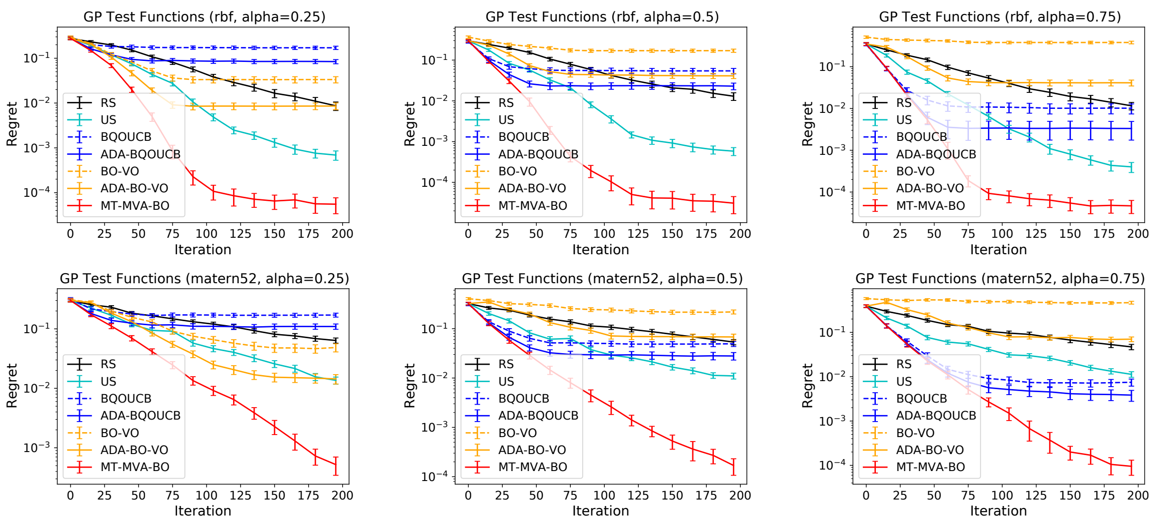

Figure 5: Average performances of multi-task optimization experiments with GP test functions in the simulator-based setting.

E.2.2 Benchmark Functions for Optimization

We conducted experiments with following benchmark functions; Mccormick (2D), Himmelblau (2D), Branin (2D), Bird (2D), Rosenbrock (2D) and Rosenbrock (3D). In the multi-task scenario, we set $\alpha = 0.5$ in all benchmarks. In the multi-objective and constraint optimization scenario, we multiplied -1 to the function values of benchmarks except for Bird as preprocessing. Furthermore, We defined h as the 75-th percentile of F_2 values in each benchmark. Figure 8 shows the results with these functions. We also show results of the simulator-based setting in Figure 9.

E.2.3 Sensitivity to the choice of β_t

In this subsection, we analyzed the effect of the choice β_t. We conducted experiments in the same settings as section E.2.1. Figure 10 shows the results with various β_t. The result suggests that small β_t tends to be good performance. In the multi-task and the multi-objective scenarios, the performance differences between these β_t seem trivial, however, it is not in constraint scenario. In the constraint scenario, the choice of β_t directly affects the classification whether the solution is feasible or not. Large β_t makes this classification rule too conservative and induces poor performance in the early stage of optimizations.

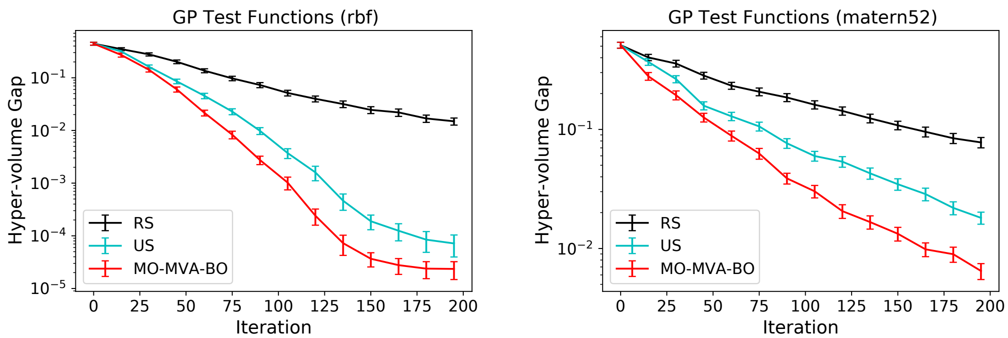

Figure 6: Average performances of multi-objective optimization experiments with GP test functions in the simulator-based setting.

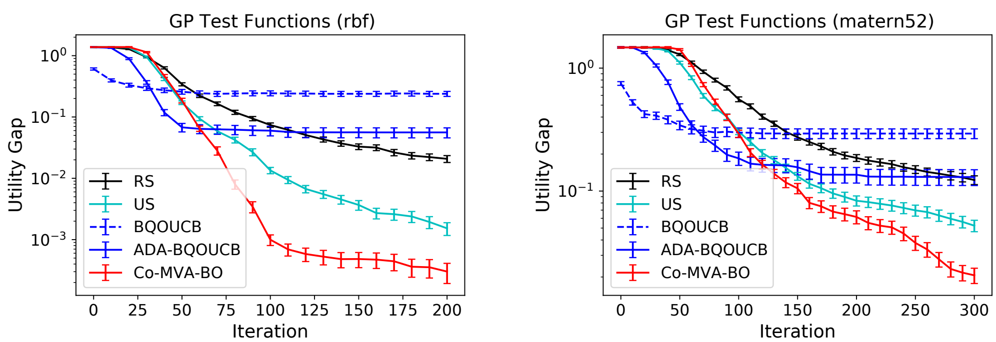

Figure 7: Average performances of constraint optimization experiments with GP test functions in the simulator-based setting.

E.2.4 Noisy Input Setting

In this subsection, we conducted experiments with GP test functions with noisy-input setting described in section 3.2. First, we divided $[-0.5, 0.5]^2$ into 20 uniformly spaced grid points in each dimension and set these grid points as $\mathcal{X}$. Furthermore, we divided $[-0.5, 0.5]^2$ into 10 uniformly spaced grid points and set these grid points as Δ. We defined $p(\boldsymbol{\xi}) = \phi(\boldsymbol{\xi}_1)\phi(\boldsymbol{\xi}_2)/Z$ and $Z = \sum_{\boldsymbol{\xi}\in\Delta} \phi(\boldsymbol{\xi}_1)\phi(\boldsymbol{\xi}_2)$, where ϕ is the density function of the standard Normal distribution. To create test functions, we first divided $[-1.0, 1.0]^2$ into 25 uniformly spaced grid points in each dimension and generated the sample path from the GP prior. After that, we created the 50 test functions in the same way of §5.1, and conducted 10 runs for each function and reported the average performance of a total of 500 experiments. Other settings are same as §E.2.1. Figure 11 shows the results of experiments in the noisy-input setting.

E.3 Real-data Experiments

E.3.1 Newsvendor Problem under Dynamic Consumer Substitution

The goal of this problem is to find the optimal inventory level of products to maximize the profit, which is computed by a stochastic simulation. Given the initial inventory levels of products which is noted as $\boldsymbol{x}$, and the purchasing behaver of customers which is noted as $\boldsymbol{w}$, the simulator outputs the profit $f(\boldsymbol{x}, \boldsymbol{w})$ after I customers visit. The details of the simulation process are in section 6.6 of Toscano-Palmerin and Frazier (2018). In our experiment, we considered the two products setting whose costs of products are $c_1 = 4$ and $c_2 = 13$, and the prices are $p_1 = 10$ and $p_2 = 23$, respectively, and chose $I = 50$. Furthermore, we divided $[0, I] \times [0, I]$ into 50 uniformly spaced grids in each dimension, and set these grid points as $\mathcal{X}$. We also divided $[w_1^{\mathrm{st}}, w_1^{\mathrm{ed}}] \times [w_2^{\mathrm{st}}, w_2^{\mathrm{ed}}]$ into 10 uniformly spaced grids, where $[w_j^{\mathrm{st}}, w_j^{\mathrm{ed}}]$ is the 99.9% confidence interval of w_j, and set these grid points as Ω. We used ARD 5/2-Matérn kernel $k((\boldsymbol{x}, \boldsymbol{w}), (\boldsymbol{x}', \boldsymbol{w}')) = \sigma_{\mathrm{ker}}^2(1 + \sqrt{5}r + \frac{5}{3}r^2) \exp(-\sqrt{5}r)$, where

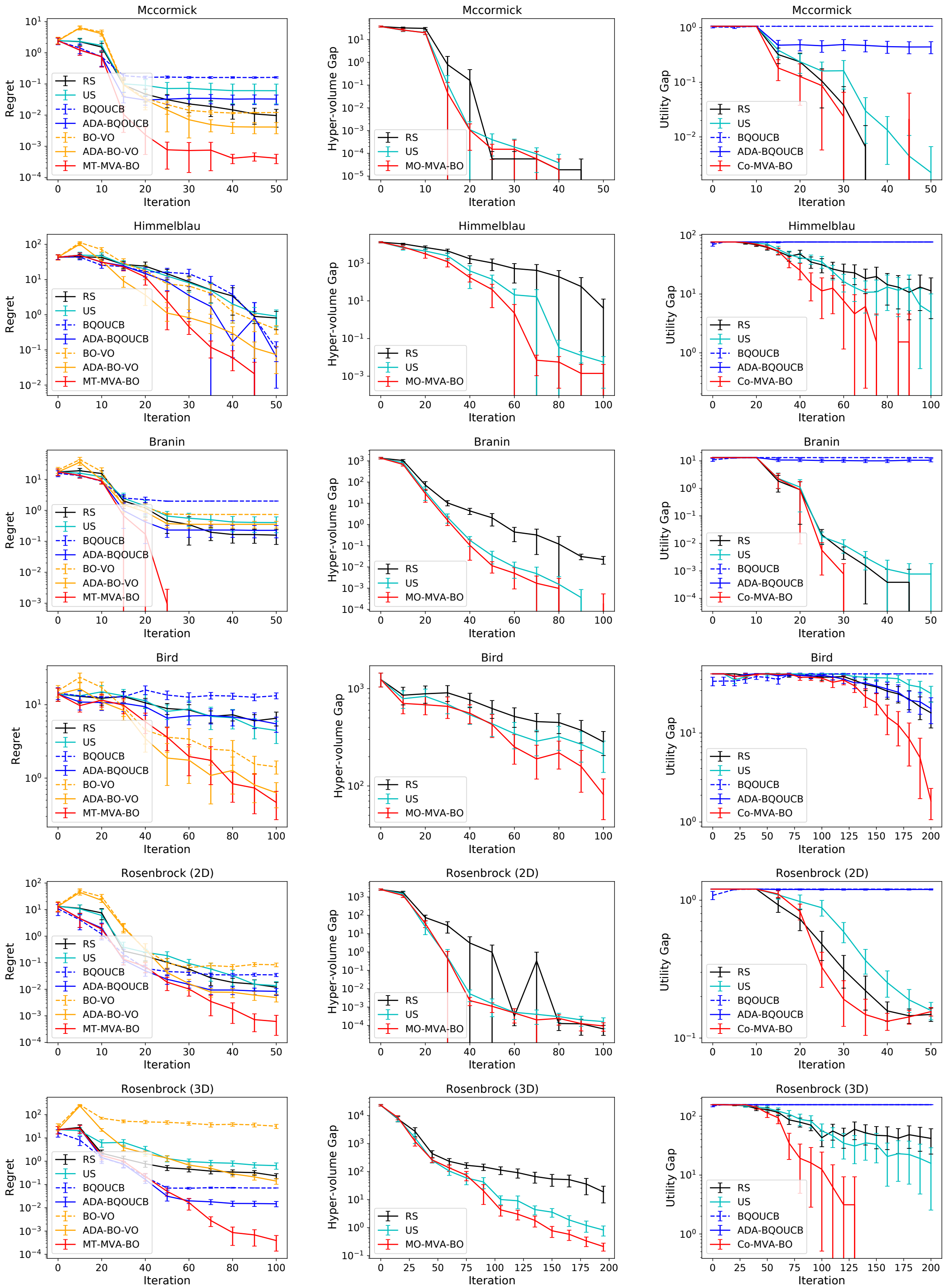

Figure 8: Average performance in 50 simulations of experiments with benchmark functions. The left, middle and right figures represent the multi-task, multi-objective and constraint optimization experiments, respectively.

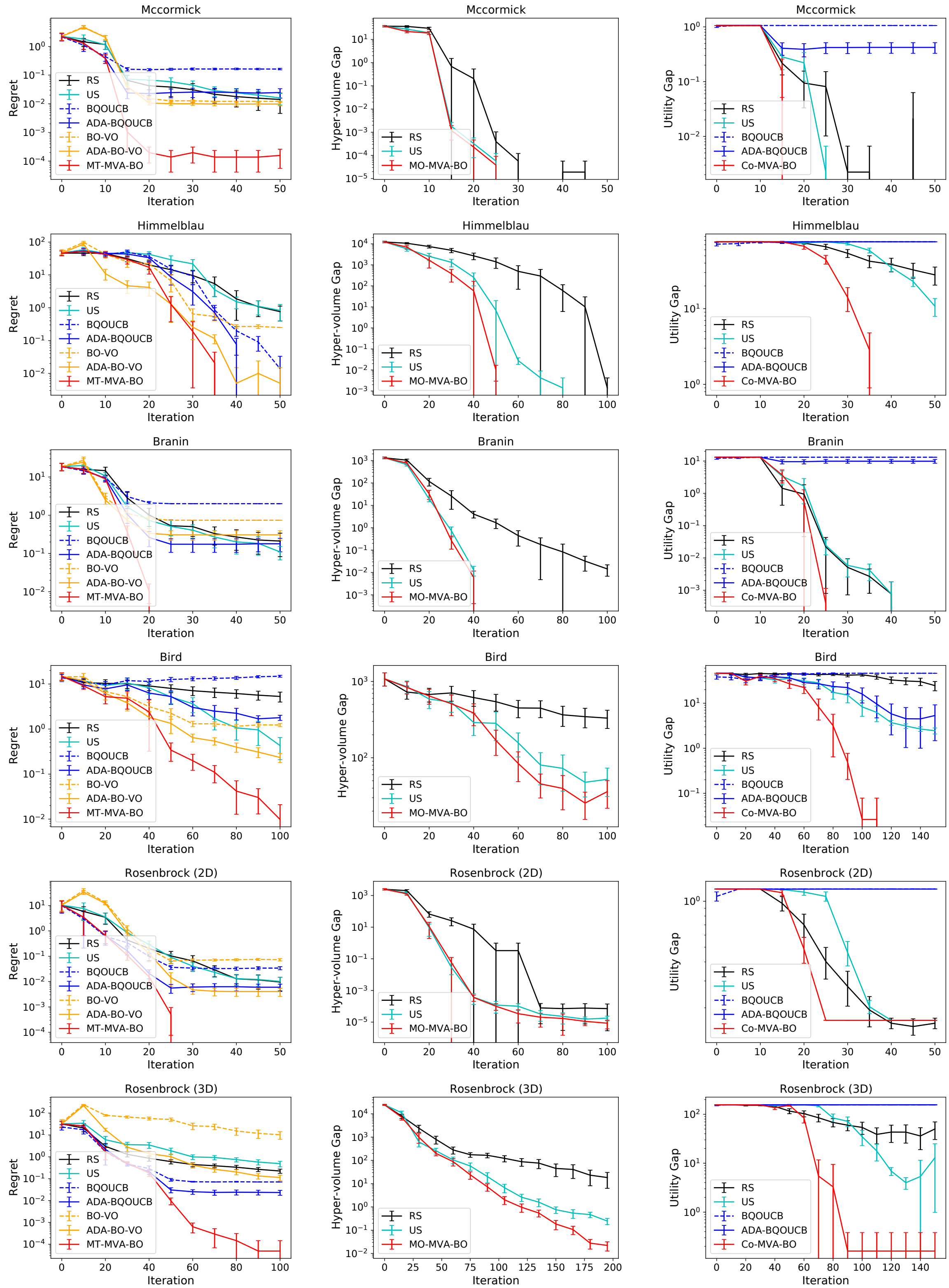

Figure 9: Average performance of experiments with benchmark functions in the simulator-based setting.

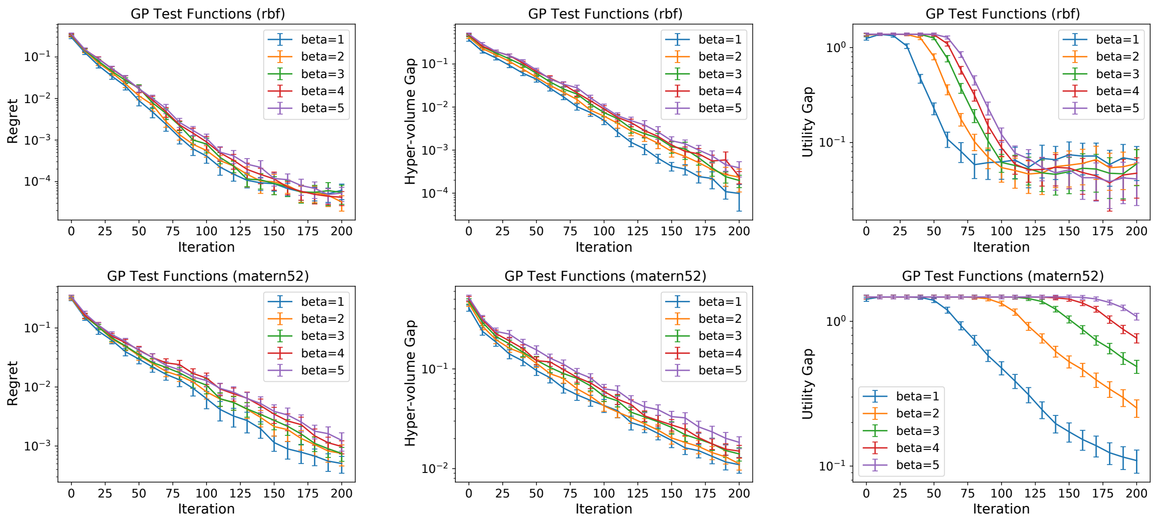

Figure 10: Average performances of experiments with various β_t. The left, middle and right figures represent the multi-task ($\alpha = 0.5$), multi-objective and constraint optimization experiments, respectively.

$r = \sqrt{\sum_{j=1}^{d_1} (\boldsymbol{x}_j - \boldsymbol{x}'_j)^2 / l_j^{(x)2} + \sum_{j=1}^{d_2} (\boldsymbol{w}_j - \boldsymbol{w}'_j)^2 / l_j^{(w)2}}$, and tuned all hyperparameters by maximizing marginal likelihood at every 10 steps. Furthermore, we set $\alpha = 0.5$ in the multi-task scenario.

E.3.2 Portfolio Optimization Problem

The goal of this problem is to find the optimal hyperparameters of the trading strategy to maximize the average daily return over a period of four years, which is computed in the simulation with CVXPortfolio (Boyd et al., 2017). A control parameter $\boldsymbol{x}$ corresponds to three parameters; a risk and a trade aversion parameters, and a holding cost multiplier, whose domains are defined as $[0.1, 1000]$, $[5.5, 8]$ and $[0.1, 100]$, respectively. A environmental parameter $\boldsymbol{w}$ corresponds to two parameters; a bid-ask spread and a borrow cost, which are assumed as random variables whose densities are uniform over $[10^{-4}, 10^{-2}]$ and $[10^{-4}, 10^{-3}]$, respectively. To simplify experiments, we respectively divided the domains of control parameters into 10 uniformly spaced grid points and set these grid points as $\mathcal{X}$. We also applied the same procedure to the domains of environmental parameters to define Ω. Furthermore, as in Cakmak et al. (2020), to avoid prohibitive costs of the simulation in the experiment, we defined the true oracle function as a surrogate function obtained as the posterior mean function of the GP, whose training data are evaluations of the actual simulator across 1000 points of Sobol sampling design (Owen, 1998). To define true oracle function, we used the ARD Gaussian kernel whose hyperparameters are tuned by maximizing the marginal likelihood, and assume that it is known in all the algorithms. Furthermore, we set $\alpha = 0.25$ in the multi-task scenario.

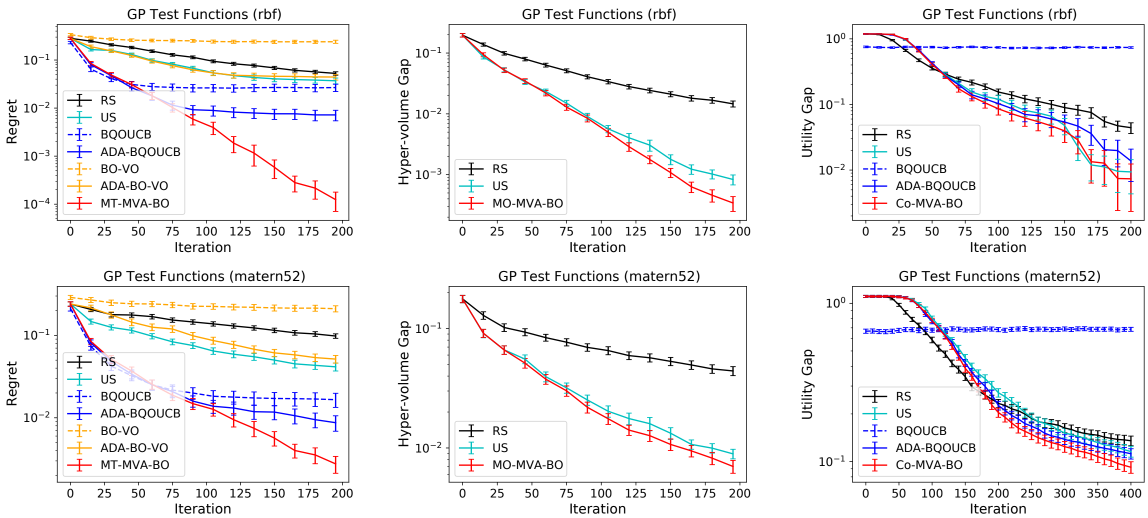

Figure 11: Average performance of noisy input experiments. The left, middle and right figures represent the multi-task ($\alpha = 0.5$), multi-objective and constraint optimization experiments, respectively. The top and bottom figures show the results of Gaussian and 5/2-Matérn kernel, respectively.

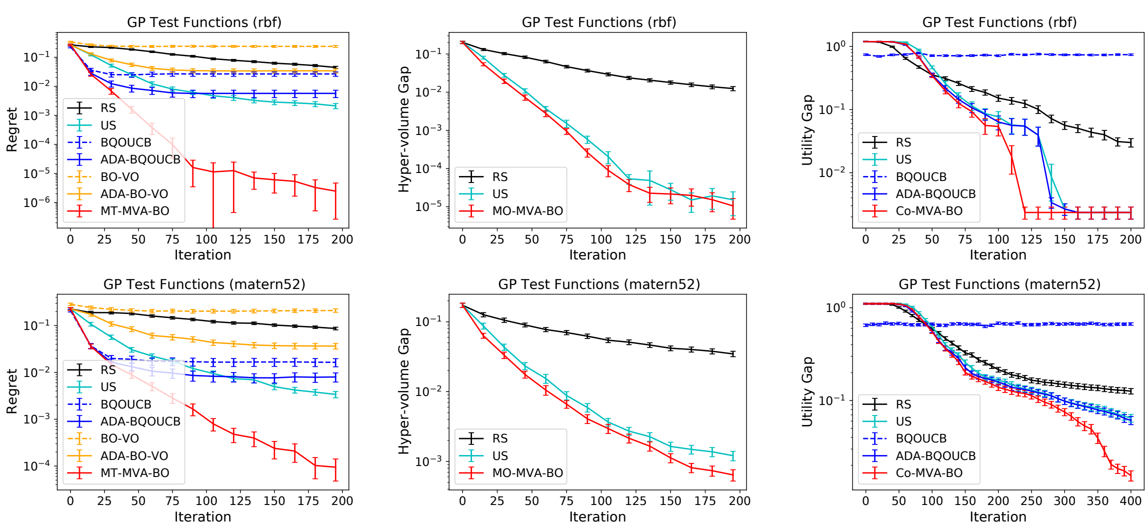

Figure 12: Average performance of noisy input experiments in the simulator-based setting.

References

Stephen Boyd, Enzo Busseti, Steven Diamond, Ronald Kahn, Kwangmoo Koh, Peter Nystrup, and Jan Speth. Multi-period trading via convex optimization. 3, 04 2017. doi: 10.1561/2400000023.

Sait Cakmak, Raul Astudillo, Peter Frazier, and Enlu Zhou. Bayesian optimization of risk measures. *arXiv preprint arXiv:2007.05554*, 2020.

Agathe Girard. *Approximate methods for propagation of uncertainty with Gaussian process models.* PhD thesis, Citeseer, 2004.

José Miguel Hernández-Lobato, Michael A Gelbart, Ryan P Adams, Matthew W Hoffman, and Zoubin Ghahramani. A general framework for constrained Bayesian optimization using information-based search. *The Journal of Machine Learning Research*, 17(1):5549–5601, 2016.

Johannes Kirschner and Andreas Krause. Information directed sampling and bandits with heteroscedastic noise. In *Proc. International Conference on Learning Theory (COLT)*, July 2018.

Hsiang-Tsung Kung, Fabrizio Luccio, and Franco P Preparata. On finding the maxima of a set of vectors. *Journal of the ACM (JACM)*, 22(4):469–476, 1975.

Art B Owen. Scrambling Sobol'and Niederreiter–Xing points. *Journal of complexity*, 14(4):466–489, 1998.

Niranjan Srinivas, Andreas Krause, Sham M. Kakade, and Matthias W. Seeger. Gaussian process optimization in the bandit setting: No regret and experimental design. In *Proceedings of the 27th International Conference on Machine Learning (ICML-10), June 21-24, 2010, Haifa, Israel*, pages 1015–1022, 2010. URL `https://icml.cc/Conferences/2010/papers/422.pdf`.

Yanan Sui, Alkis Gotovos, Joel Burdick, and Andreas Krause. Safe exploration for optimization with Gaussian processes. In *International Conference on Machine Learning*, pages 997–1005, 2015.

Yanan Sui, Vincent Zhuang, Joel W. Burdick, and Yisong Yue. Stagewise safe Bayesian optimization with Gaussian processes. In *Proceedings of the 35th International Conference on Machine Learning, ICML 2018, Stockholmsmässan, Stockholm, Sweden, July 10-15, 2018*, volume 80 of *Proceedings of Machine Learning Research*, pages 4788–4796, 2018. URL `http://proceedings.mlr.press/v80/sui18a.html`.

Saul Toscano-Palmerin and Peter I. Frazier. Bayesian optimization with expensive integrands. *CoRR*, abs/1803.08661, 2018. URL `http://arxiv.org/abs/1803.08661`.

Marcela Zuluaga, Andreas Krause, and Markus Püschel. e-pal: An active learning approach to the multi-objective optimization problem. *Journal of Machine Learning Research*, 17(104):1–32, 2016. URL `http://jmlr.org/papers/v17/15-047.html`.